

ϵ'_K/ϵ_K and $K \rightarrow \pi\nu\bar{\nu}$ in a two-Higgs doublet model

Chuan-Hung Chen^{1,*} and Takaaki Nomura^{2,†}

¹*Department of Physics, National Cheng-Kung University, Tainan 70101, Taiwan*

²*School of Physics, KIAS, Seoul 02455, Korea*

(Dated: August 23, 2018)

Abstract

The Kaon direct CP violation $Re(\epsilon'_K/\epsilon_K)$ below the experimental data of a 2σ in the standard model, which is calculated using the RBC-UKQCD lattice and a large N_c dual QCD, indicates the necessity of a new physics effect. In order to resolve the insufficient $Re(\epsilon'_K/\epsilon_K)$, we study the charged-Higgs contributions in a generic two-Higgs-doublet model. If we assume that the origin of the CP-violation phase is uniquely from the Kobayashi-Maskawa (KM) phase when the constraints from the B - and K -meson mixings, $B \rightarrow X_s\gamma$, and Kaon indirect CP violating parameter ϵ_K are simultaneously taken into account, it is found that the Kaon direct CP violation through the charged-Higgs effects can reach $Re(\epsilon'_K/\epsilon_K)_{H^\pm} \sim 8 \times 10^{-4}$. Moreover, with the constrained values of the parameters, the branching ratios of the rare $K \rightarrow \pi\nu\bar{\nu}$ decays can be $BR(K^+ \rightarrow \pi^+\nu\bar{\nu}) \sim 13 \times 10^{-11}$ and $BR(K_L \rightarrow \pi^0\nu\bar{\nu}) \sim 3.6 \times 10^{-11}$, where the results can be tested through the NA62 experiment at CERN and the KOTO experiment at J-PARC, respectively.

*Electronic address: physchen@mail.ncku.edu.tw

†Electronic address: nomura@kias.re.kr

I. INTRODUCTION

Since a large time-dependent CP asymmetry through the $B_d \rightarrow J/\Psi K_S$ mode was observed at the BaBar [1] and BELLE [2] experiments, it is certain that the origin of the observed CP violation at colliders, including the indirect (ϵ_K) and direct ($Re(\epsilon'_K/\epsilon_K)$) CP violation in the K -meson, mainly stems from the unique CP phase of the Cabibbo-Kobayashi-Maskawa (CKM) matrix [3, 4] in the standard model (SM).

Recently, the RBC-UKQCD collaboration reported the surprising lattice QCD results on the matrix elements of $K \rightarrow \pi\pi$ and $Re(\epsilon'_K/\epsilon_K)$ [5–9], where the Kaon direct CP violation and the contribution from the electroweak penguin to it are respectively given as [8, 9]:

$$Re(\epsilon'_K/\epsilon_K) = 1.38(5.15)(4.59) \times 10^{-4}, \quad Re(\epsilon'_K/\epsilon_K)_{\text{EWP}} = -(6.6 \pm 1.0) \times 10^{-4}, \quad (\text{I.1})$$

whereas the average of the NA48 [10] and KTeV [11, 12] results is $Re(\epsilon'_K/\epsilon_K) = (16.6 \pm 2.3) \times 10^{-4}$. That is, a 2.1σ below the experimental value is obtained using the lattice calculations.

Intriguingly, the recent theoretical calculations of $Re(\epsilon'_K/\epsilon_K)$ using a large N_c dual QCD approach [13, 14], which was developed by [15–19], support the RBC-UKQCD results, and the results are obtained as:

$$Re(\epsilon'_K/\epsilon_K)_{\text{SM}} = (8.6 \pm 3.2) \times 10^{-4}, \quad (B_6^{(1/2)} = B_8^{(3/2)} = 1), \quad (\text{I.2})$$

$$Re(\epsilon'_K/\epsilon_K)_{\text{SM}} = (6.0 \pm 2.4) \times 10^{-4}, \quad (B_6^{(1/2)} = B_8^{(3/2)} = 0.76), \quad (\text{I.3})$$

where $B_6^{(1/2)}$ and $B_8^{(3/2)}$ denote the non-perturbative parameters of gluon and electroweak penguin operators, respectively. It is found that both approaches obtain consistent values of $B_6^{(1/2)}$ and $B_8^{(3/2)}$ as [13]:

$$\begin{aligned} B_6^{(1/2)}(m_c) &= 0.57 \pm 0.19, \quad B_8^{(3/2)}(m_c) = 0.76 \pm 0.05 \quad (\text{RBC-UKQCD}), \\ B_6^{(1/2)} &\leq B^{(3/2)} < 1, \quad B_8^{(3/2)}(m_c) = 0.80 \pm 0.1. \quad (\text{large } N_c). \end{aligned} \quad (\text{I.4})$$

Since the main contributions to $Re(\epsilon'_K/\epsilon_K)$ in the SM are dictated by $B_6^{(1/2)}$ and $B_8^{(3/2)}$, and there is a cancellation between gluon and electroweak penguin contribution, thus, a smaller $B_6^{(1/2)}$ leads to a $Re(\epsilon'_K/\epsilon_K)_{\text{SM}}$ below the experimental value of 2σ . The small $Re(\epsilon'_K/\epsilon_K)$, which results from a QCD based approach and arises from the short-distance (SD) effects, could be compensated for by other sources in the SM, such as chromomagnetic dipole effects and long-distance (LD) final state interactions (FSIs). However, according to the recent

study in [21], the contribution to $Re(\epsilon'_K/\epsilon_K)$ from the gluonic dipole operators in the SM should be less than 10^{-4} and cannot explain the data. In addition, the conclusion about the LD contribution is still uncertain, where the authors in [20] obtained negative result, but the authors in [22] obtained $Re(\epsilon'_K/\epsilon_K) = (15 \pm 7) \times 10^{-4}$ when the SD and LD effects were considered. Hence, in spite of the large uncertainty of the current lattice calculations, if we take the RBC-UKQCD's central result, which basically includes all nonperturbative QCD effects, as the tendency of the SM, the alternative source for the insufficient $Re(\epsilon'_K/\epsilon_K)$ can be attributed to a new physics effect [23–37], which we will focus on in this study.

In rare K decays, two important unobserved processes are $K^+ \rightarrow \pi^+ \nu \bar{\nu}$ and $K_L \rightarrow \pi^0 \nu \bar{\nu}$, where the former is a CP-conserving channel, and the latter denotes a CP-violation. The NA62 experiment at CERN plans to measure the branching ratio (BR) for $K^+ \rightarrow \pi^+ \nu \bar{\nu}$, which can reach the SM result with a 10% precision [47, 48], and the KOTO experiment at J-PARC will observe the $K_L \rightarrow \pi^0 \nu \bar{\nu}$ decay [49, 50]. In addition to their sensitivity to new physics, their importance is that the SM predictions are theoretically clean, where the QCD corrections at the next-to-leading-order (NLO) [38–40] and NNLO [41–43] and the electroweak corrections at the NLO [44–46] have been calculated. The SM predictions are [23]:

$$BR(K^+ \rightarrow \pi^+ \nu \bar{\nu}) = (9.11 \pm 0.72) \times 10^{-11}, \quad (\text{I.5})$$

$$BR(K_L \rightarrow \pi^0 \nu \bar{\nu}) = (3.00 \pm 0.31) \times 10^{-11}, \quad (\text{I.6})$$

whereas the current experimental situations are $BR(K^+ \rightarrow \pi^+ \nu \bar{\nu})^{\text{exp}} = (17.3_{-10.5}^{+11.5}) \times 10^{-11}$ [51] and $BR(K_L \rightarrow \pi^0 \nu \bar{\nu})^{\text{exp}} < 2.6 \times 10^{-8}$ [52]. Recently, NA62 reported its first result using the 2016 taken data. It was found that one candidate event of $K^+ \rightarrow \pi^+ \nu \bar{\nu}$ is observed and that the upper bound of BR is given by $BR(K^+ \rightarrow \pi^+ \nu \bar{\nu}) < 14 \times 10^{-10}$ at a 95% confidence level (CL) [53].

To pursue new physics contributions to the $Re(\epsilon'_K/\epsilon_K)$ and rare K decays, in this work, we investigate the influence of a charged-Higgs in a generic two-Higgs-doublet model (2HDM), i.e., the type-III 2HDM, where global symmetry is not imposed on the Yukawa sector. As a result, flavor changing neutral currents (FCNCs) in such models can arise at the tree level. To reasonably suppress the tree-level FCNCs for the purpose of satisfying the constraints from the B and K systems, such as $\Delta M_{B_d, B_s}$, $B \rightarrow X_s \gamma$, ΔM_K , and ϵ_K , we can adopt the so-called Cheng-Sher ansatz [54], where the neutral scalar-mediated flavor-changing

effects are dictated by the square-root of the mass product of the involved flavors, denoted by $\sqrt{m_{f_i} m_{f_j}}/v$. Thus, we can avoid extreme fine-tuning of the free parameters when they contribute to the rare K and B decays. The alternative approach for suppressing the FCNCs using 't Hooft's naturalness criterion [55] can be found in [56], where more related flavor phenomena were studied in detail.

From a phenomenological viewpoint, the reasons why the charged-Higgs effects in the type-III 2HDM are interesting can be summarized as follows: firstly, $Re(\epsilon'_K/\epsilon_K)$ and $K \rightarrow \pi\nu\bar{\nu}$ in the SM are all dictated by the product of the CKM matrix elements V_{ts}^* and V_{td} . The same CKM factor automatically appears in the charged-Higgs Yukawa couplings without introducing any new weak CP-violation phase; thus, we can avoid the strict limits from the time-dependent CP asymmetries in the B_d and B_s systems. Secondly, unlike the type-II 2HDM, where the charged-Higgs mass is bounded to be $m_{H^\pm} > 580$ GeV via the $B \rightarrow X_s\gamma$ decay [57, 58], the charged-Higgs in the type-III model can be much lighter than that in the type-II model, due to the modification of the Yukawa couplings [58]. Thirdly, a peculiar unsuppressed Yukawa coupling $\sqrt{m_c/m_t}V_{cq'}/V_{tq'}\chi_{ct}^{u*}$ (see the later discussions), which originates from the FCNCs, also appears in the charged-Higgs couplings to the top-quark and down-type quarks [58, 59]. The effects play a key role in enhancing $Re(\epsilon'_K/\epsilon_K)$ and $K \rightarrow \pi\nu\bar{\nu}$ in this model. Fourthly, the charged-Higgs effects can naturally provide the lepton-flavor universality violation and can be used to resolve the puzzles in the semileptonic B decays, such as $R(D)$, $R(K^{(*)})$, and large $BR(B_u^- \rightarrow \tau\bar{\nu})$ [58–67].

Since the charged-Higgs effects have a strong correlation with different phenomena, the new free parameters are not constrained by only one physical observable. Therefore, the involved new parameters are strictly limited and cannot be arbitrarily free. It is found that when the constraints of $\Delta B = 2$, $\Delta K = 2$, $B \rightarrow X_s\gamma$, and ϵ_K are simultaneously taken into account, the charged-Higgs contribution to the direct CP violation of K -meson can reach $Re(\epsilon'_K/\epsilon_K)_{H^\pm} \sim 8 \times 10^{-4}$ (not including the SM contribution), and the BR for $K^+ \rightarrow \pi^+\nu\bar{\nu}$ can be $BR(K^+ \rightarrow \pi^+\nu\bar{\nu}) \sim 13 \times 10^{-11}$, while $BR(K_L \rightarrow \pi^0\nu\bar{\nu}) \sim 3.6 \times 10^{-11}$.

The paper is organized as follows: In Section II, we briefly review the charged-Higgs and neutral scalar Yukawa couplings to the fermions with the Cheng-Sher ansatz in the type-III 2HDM. In Section III, we formulate ΔM_K , ϵ_K , and $Re(\epsilon'_K/\epsilon_K)$ in the 2HDM. The charged-Higgs contributions to the rare $K \rightarrow \pi\nu\bar{\nu}$ decays are shown in Section IV. The detailed numerical analysis is shown in Section V, where the constraints from $\Delta M_{B_d, B_s}$, $B \rightarrow X_s\gamma$,

ΔM_K , and ϵ_K are included. A conclusion is given in Section V.

II. CHARGED AND NEUTRAL HIGGS COUPLINGS TO THE QUARKS AND LEPTONS

In this section, we summarize the Yukawa couplings of the neutral Higgses and charged-Higgs to the quarks and leptons in the generic 2HDM. The Yukawa couplings without imposing extra global symmetry can be in general written as:

$$\begin{aligned}
-\mathcal{L}_Y &= \bar{Q}_L Y_1^d D_R H_1 + \bar{Q}_L Y_2^d D_R H_2 + \bar{Q}_L Y_1^u U_R \tilde{H}_1 + \bar{Q}_L Y_2^u U_R \tilde{H}_2 \\
&+ \bar{L} Y_1^\ell \ell_R H_1 + \bar{L} Y_2^\ell \ell_R H_2 + H.c. ,
\end{aligned} \tag{II.1}$$

where all flavor indices are hidden; $P_{R(L)} = (1 \pm \gamma_5)/2$; Q_L and L_L are the $SU(2)_L$ quark and lepton doublets, respectively; f_R ($f = U, D, \ell$) denotes the singlet fermion; $Y_{1,2}^f$ are the 3×3 Yukawa matrices, and $\tilde{H}_i = i\tau_2 H_i^*$. There are two CP-even scalars, one CP-odd pseudoscalar, and two charged-Higgs particles in the 2HDM, and the relations between physical and weak states can be expressed as:

$$\begin{aligned}
h &= -s_\alpha \phi_1 + c_\alpha \phi_2 , \\
H &= c_\alpha \phi_1 + s_\alpha \phi_2 , \\
H^\pm(A) &= -s_\beta \phi_1^\pm(\eta_1) + c_\beta \phi_2^\pm(\eta_2) ,
\end{aligned} \tag{II.2}$$

where $\phi_i(\eta_i)$ and η_i^\pm denote the real (imaginary) parts of the neutral and charged components of H_i , respectively; $c_\alpha(s_\alpha) = \cos \alpha(\sin \alpha)$, $c_\beta = \cos \beta = v_1/v$, and $s_\beta = \sin \beta = v_2/v$, v_i are the vacuum expectation values (VEVs) of H_i , and $v = \sqrt{v_1^2 + v_2^2} \approx 246$ GeV. In this study, h is the SM-like Higgs while H , A , and H^\pm are new particles in the 2HDM.

Introducing the unitary matrices $V_{L,R}^f$ to diagonalize the quark and lepton mass matrices, the Yukawa couplings of scalars H and A can then be obtained as:

$$\begin{aligned}
-\mathcal{L}_Y^{H,A} &= \bar{u}_L \left[\frac{s_\alpha}{vs_\beta} \mathbf{m}_u + \frac{s_{\beta\alpha}}{s_\beta} \mathbf{X}^u \right] u_R H + \bar{d}_L \left[\frac{c_\alpha}{vc_\beta} \mathbf{m}_d - \frac{s_{\beta\alpha}}{c_\beta} \mathbf{X}^d \right] d_R H \\
&+ \bar{\ell}_L \left[\frac{c_\alpha}{vc_\beta} \mathbf{m}_\ell - \frac{s_{\beta\alpha}}{c_\beta} \mathbf{X}^\ell \right] \ell_R H + i\bar{u}_L \left[-\frac{c_\beta}{v} \mathbf{m}_u + \frac{\mathbf{X}^u}{s_\beta} \right] u_R A \\
&+ i\bar{d}_L \left[-\frac{t_\beta}{v} \mathbf{m}_d + \frac{\mathbf{X}^d}{c_\beta} \right] d_R A + i\bar{\ell}_L \left[-\frac{t_\beta}{v} \mathbf{m}_\ell + \frac{\mathbf{X}^\ell}{c_\beta} \right] \ell_R A + H.c. ,
\end{aligned} \tag{II.3}$$

where \mathbf{m}_f is the diagonalized fermion mass matrix; $t_\beta = s_\beta/c_\beta = v_2/v_1$; $c_{\beta\alpha} = \cos(\beta - \alpha)$; $s_{\beta\alpha} = \sin(\beta - \alpha)$, and \mathbf{X}^f s are defined as:

$$\mathbf{X}^u = V_L^u \frac{Y_1^u}{\sqrt{2}} V_R^{u\dagger}, \quad \mathbf{X}^d = V_L^d \frac{Y_2^d}{\sqrt{2}} V_R^{d\dagger}, \quad \mathbf{X}^\ell = V_L^\ell \frac{Y_2^\ell}{\sqrt{2}} V_R^{\ell\dagger}. \quad (\text{II.4})$$

We can also obtain the Higgs Yukawa couplings; however, it is found that the associated X^f terms are always related to $c_{\alpha\beta}$, which is strictly bound by the current precision Higgs data. For simplicity, we take the alignment limit with $c_{\alpha\beta} = 0$ in the following analysis. Thus, the Higgs couplings are the same as those in the SM. The charged-Higgs Yukawa couplings to fermions are found as:

$$\begin{aligned} -\mathcal{L}_Y^{H^\pm} &= \sqrt{2} \bar{d}_L V^\dagger \left[-\frac{1}{vt_\beta} \mathbf{m}_u + \frac{\mathbf{X}^u}{s_\beta} \right] u_R H^- \\ &+ \sqrt{2} \bar{u}_L V \left[-\frac{t_\beta}{v} \mathbf{m}_d + \frac{\mathbf{X}^d}{c_\beta} \right] d_R H^+ \\ &+ \sqrt{2} \bar{\nu}_L \left[-\frac{t_\beta}{v} \mathbf{m}_\ell + \frac{\mathbf{X}^\ell}{c_\beta} \right] \ell_R H^+ + H.c., \end{aligned} \quad (\text{II.5})$$

where $V \equiv V_L^u V_L^{d\dagger}$ stands for the CKM matrix. Except the factor $\sqrt{2}$ and CKM matrix, the Yukawa couplings of charged Higgs are the same as those of pseudoscalar A .

From Eq. (II.3), the FCNCs at the tree level can be induced through the \mathbf{X}^f terms. To suppress the tree-induced $\Delta F = 2$ ($F = K, B_{d(s)}, D$) processes, we employ the Cheng-Sher ansatz [54] as:

$$X_{ij}^f = \frac{\sqrt{m_{f_i} m_{f_j}}}{v} \chi_{ij}^f, \quad (\text{II.6})$$

where χ_{ij}^f are the new free parameters. With the Cheng-Sher ansatz, the Yukawa couplings of scalars H and A to the down-type quarks can be straightforwardly obtained as:

$$-\mathcal{L}_Y^{H,A} = \frac{t_\beta}{v} \bar{d}_{iL} \left[m_{d_i} \delta_{ij} - \frac{\sqrt{m_{d_i} m_{d_j}}}{s_\beta} \chi_{ij}^d \right] d_{jR} (H - iA) + H.c., \quad (\text{II.7})$$

where the CKM matrix elements are not involved.

Since the charged-Higgs interactions are associated with the CKM matrix elements, the couplings involving the third generation quarks may not be small; therefore, for the K -meson decays, it is worth analyzing the charged-Higgs Yukawa couplings of the d - and s -quark to the top-quark, i.e., tdH^+ and tsH^+ . According to Eq. (II.5), the $t_R d_L H^+$ coupling can be

written and simplified as

$$\begin{aligned}
t_R d_L H^+ &: \frac{\sqrt{2}}{v} \left[\left(\frac{1}{t_\beta} - \frac{\chi_{tt}^{u*}}{s_\beta} \right) m_t V_{td} - \frac{\sqrt{m_t m_c}}{s_\beta} \chi_{ct}^{u*} V_{cd} - \frac{\sqrt{m_t m_u}}{s_\beta} \chi_{ut}^{u*} V_{ud} \right] \\
&\approx \sqrt{2} \frac{m_t}{v} V_{td} \left(\frac{1}{t_\beta} - \frac{\chi_{td}^L}{s_\beta} \right), \quad \chi_{td}^L = \chi_{tt}^{u*} + \sqrt{\frac{m_c}{m_t}} \frac{V_{cd}}{V_{td}} \chi_{ct}^{u*},
\end{aligned} \tag{II.8}$$

where we have dropped the χ_{ut}^{u*} term because its coefficient is a factor of 4 smaller than the χ_{ct}^{u*} term. In addition to the m_t enhancement, the effect associated with χ_{ct}^u is $\sqrt{m_c/m_t} |V_{cd}/V_{td}| \chi_{ct}^{u*} \approx 2.4 \chi_{ct}^{u*}$, which is in principle not suppressed. Intriguingly, the charged-Higgs coupling is comparable to the SM gauge coupling of $(g/\sqrt{2})V_{td}$. Because $m_d V_{td} \ll \sqrt{m_s m_d} V_{ts} \ll \sqrt{m_b m_d} V_{tb}$, the $t_L d_R H^+$ coupling can be approximated as:

$$t_L d_R H^+ : -\sqrt{2} \frac{m_b t_\beta}{v} \sqrt{\frac{m_d}{m_b}} \frac{\chi_{bd}^d V_{tb}}{s_\beta}. \tag{II.9}$$

Although there is no V_{td} suppression, because $\chi_{bd}^d \sim O(10^{-2})$ is constrained by the B_d mixing [58], the coupling of $t_L d_R H^+$ is somewhat smaller than that of $t_R d_L H^+$, even with the large value of t_β , e.g. $t_\beta \sim 50$. Using $m_t |V_{ts}| \sim 6.72 \text{ GeV} < \sqrt{m_c m_t} V_{cs} \sim 14.8 \text{ GeV}$ and $m_s V_{ts} \ll \sqrt{m_s m_b} V_{tb} \sim 0.66 \text{ GeV}$, the $ts H^+$ coupling can be similarly obtained as:

$$\begin{aligned}
t_R s_L H^+ &: \sqrt{2} \frac{m_t}{v} V_{ts} \left(\frac{1}{t_\beta} - \frac{\chi_{ts}^L}{s_\beta} \right), \quad \chi_{ts}^L = \chi_{tt}^{u*} + \sqrt{\frac{m_c}{m_t}} \frac{V_{cs}}{V_{ts}} \chi_{ct}^{u*}, \\
t_L s_R H^+ &: -\sqrt{2} \frac{m_b t_\beta}{v} \sqrt{\frac{m_s}{m_b}} \frac{\chi_{bs}^d V_{tb}}{s_\beta}.
\end{aligned} \tag{II.10}$$

The detailed analysis for the other charged-Higgs couplings can be found in [58]. In sum, the charged-Higgs couplings to the $d(s)$ - and top-quark in the type-III 2HDM can be formulated as:

$$\mathcal{L}_Y^{H^\pm} \supset \frac{\sqrt{2}}{v} V_{tq'} \bar{t} (m_t \zeta_{tq'}^u P_L - m_b \zeta_{tq'}^d P_R) q' H^\pm + H.c., \tag{II.11}$$

where the parameters ζ_{ij}^f are defined as:

$$\begin{aligned}
\zeta_{tq'}^u &= \frac{1}{t_\beta} - \frac{\chi_{tq'}^L}{s_\beta}, \quad \chi_{tq'}^L = \chi_{tt}^{u*} + \sqrt{\frac{m_c}{m_t}} \frac{V_{cq'}}{V_{tq'}} \chi_{ct}^{u*}, \\
\zeta_{tq'}^d &= t_\beta \sqrt{\frac{m_{q'}}{m_b}} \frac{V_{tb}}{V_{tq'}} \frac{\chi_{bq'}^d}{s_\beta}.
\end{aligned} \tag{II.12}$$

For the lepton sector, we use the flavor-conserving scheme with $\mathbf{X}_{ij}^\ell = (m_{\ell_i}/v) \chi_{\ell_i}^\ell \delta_{\ell_i \ell_j}$, i.e. $\chi_{\ell_i \ell_j}^\ell = \chi_{\ell_i}^\ell \delta_{\ell_i \ell_j}$; as a result, the Yukawa couplings of H^\pm to the leptons can be expressed as:

$$\mathcal{L}_{Y,\ell}^{H^\pm} = \sqrt{2} \frac{\tan \beta m_\ell}{v} \zeta_\ell^\ell \bar{\nu}_\ell P_R \ell H^\pm + H.c., \tag{II.13}$$

with $\zeta_\ell^\ell = 1 - \chi_\ell^\ell/s_\beta$. The suppression factor m_ℓ/v could be moderated using a large value of $\tan\beta$. In this work, we use the interactions shown in Eqs. (II.7), (II.11), and (II.13) to study the influence on the $K^0 - \bar{K}^0$ mixing ΔM_K , ϵ_K , ϵ'_K/ϵ_K , and $K \rightarrow \pi\nu\bar{\nu}$ decays.

III. FORMULATIONS OF ΔM_K , ϵ_K , AND ϵ'_K/ϵ_K IN THE GENERIC 2HDM

A. ΔM_K and ϵ_K

To study the new physics contributions to ΔM_K and ϵ_K , we follow the notations in [69] and write the effective Hamiltonian for $\Delta S = 2$ as:

$$\mathcal{H}^{\Delta S=2} = \frac{G_F^2}{16\pi^2} m_W^2 \sum_i V_{\text{CKM}}^i C_i(\mu) Q_i, \quad (\text{III.1})$$

where V_{CKM}^i are the involved CKM matrix elements; $C_i(\mu)$ are the Wilson coefficients at the μ scale, and the relevant operators Q_i are given as:

$$\begin{aligned} Q_1^{VLL} &= (\bar{s}^\alpha \gamma_\mu P_L d^\alpha) (\bar{s}^\beta \gamma^\mu P_L d^\beta), \\ Q_1^{LR} &= (\bar{s}^\alpha \gamma_\mu P_L d^\alpha) (\bar{s}^\beta \gamma^\mu P_R d^\beta), \\ Q_2^{LR} &= (\bar{s}^\alpha P_L d^\alpha) (\bar{s}^\beta P_R d^\beta), \\ Q_1^{SLL} &= (\bar{s}^\alpha P_L d^\alpha) (\bar{s}^\beta P_L d^\beta), \\ Q_2^{SLL} &= (\bar{s}^\alpha \sigma_{\mu\nu} P_L d^\alpha) (\bar{s}^\beta \sigma^{\mu\nu} P_L d^\beta). \end{aligned} \quad (\text{III.2})$$

The operators Q_1^{VRR} and Q_i^{SRR} can be obtained from Q_1^{VLL} and Q_i^{SLL} by switching P_R and P_L , respectively.

In the type-III 2HDM, the $\Delta S = 2$ process can arise from the H/A -mediated tree FCNCs and the H^\pm -mediated box diagrams, for which the representative Feynman diagrams are sketched in Fig. 1. According to the interactions in Eq. (II.7), the H/A -induced effective Hamiltonian can be expressed as:

$$\mathcal{H}_S^{\Delta S=2} = -\frac{G_F^2}{16\pi^2} m_W^2 [C_{S1}^{SLL} Q_1^{SLL} + C_{S1}^{SRR} Q_1^{SRR} + C_{S2}^{LR} Q_2^{LR}], \quad (\text{III.3})$$

where the subscript S denotes the scalar and pseudoscalar contributions. Clearly, no CKM matrix elements are involved in the tree FCNCs. Since the involved operators are $Q_1^{SLL, SRR}$

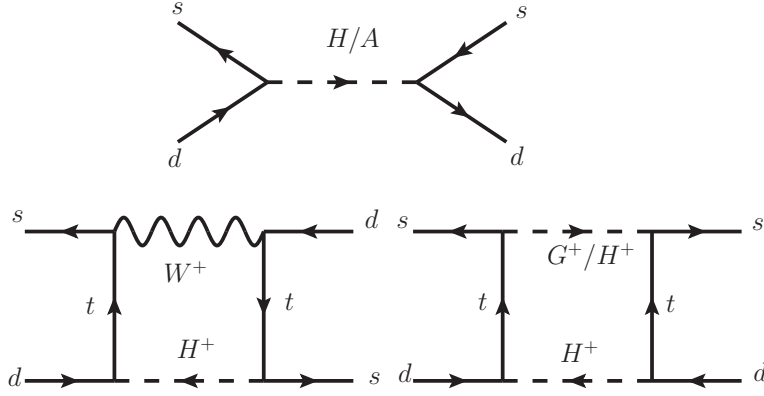


FIG. 1: Sketched Feynman diagrams for the $\Delta S = 2$ process.

and Q_2^{LR} , the corresponding Wilson coefficients at the μ_S scale are obtained as:

$$\begin{aligned}
C_{S1}^{SLL} &= r_S \left(\frac{1}{m_H^2} - \frac{1}{m_A^2} \right) (\chi_{ds}^{d*})^2, \\
C_{S1}^{SRR} &= r_S \left(\frac{1}{m_H^2} - \frac{1}{m_A^2} \right) (\chi_{sd}^d)^2, \\
C_{S2}^{LR} &= r_S \left(\frac{1}{m_H^2} + \frac{1}{m_A^2} \right) 2\chi_{sd}^d \chi_{ds}^{d*}, \\
r_S &= \frac{4\sqrt{2}\pi^2 \tan^2 \beta \sqrt{x_d x_s}}{G_F s_\beta} \approx 1.0 \times 10^3 \left(\frac{\tan^2 \beta}{50^2 s_\beta} \right), \tag{III.4}
\end{aligned}$$

with $x_q = m_q^2/m_W^2$. It can be seen from r_S that although the H/A effects are suppressed by $m_d m_s/m_W^2$, due to the $\tan \beta$ enhancement, the ΔM_K through the intermediates of H and A becomes sizable. We then can use the measured ΔM_K to bound the parameters χ_{sd}^d and χ_{ds}^{d*} . If we take $m_H = m_A$ and $\chi_{sd}^d = \chi_{ds}^{d*}$, it can be seen that $C_{S1}^{SLL} = C_{S1}^{SRR} = 0$ and that $C_{S2}^{LR} \propto \chi_{sd}^d \chi_{ds}^{d*} = |\chi_{sd}^d|^2$ is a real parameter; under this condition, ϵ_K that has arisen from the neutral scalars will be suppressed.

From the charged-Higgs interactions in Eq. (II.11), we find that with the exception of Q_2^{SLL} , the W^\pm - H^\pm , G^\pm - H^\pm , and H^\pm - H^\pm box diagrams can induce all operators shown in Eq. (III.2); the associated CKM matrix element factor is $V_{\text{CKM}}^i = (V_{ts}^* V_{td})^2$, and the Wilson

coefficients at the $\mu = m_{H^\pm}$ scale can be expressed as:

$$\begin{aligned}
C_{H^\pm 1}^{VLL} &= 4 \left(2y_t^2 I_1^{WH}(y_t, y_W) + x_t y_t I_2^{WH}(y_t, y_W) \right) \zeta_{ts}^{u*} \zeta_{td}^u + 2x_t y_t (\zeta_{ts}^{u*} \zeta_{td}^u)^2 I_1^{HH}(y_t), \\
C_{H^\pm 1}^{VRR} &= 2x_b y_b (\zeta_{ts}^{d*} \zeta_{td}^d)^2 I_1^{HH}(y_t), \\
C_{H^\pm 1}^{LR} &= 4x_b y_t (\zeta_{ts}^{u*} \zeta_{td}^u) (\zeta_{ts}^{d*} \zeta_{td}^d) I_1^{HH}(y_t), \\
C_{H^\pm 2}^{LR} &= -8 \frac{m_b^2}{m_t^2} (\zeta_{ts}^{d*} \zeta_{td}^d) \left(x_t y_t^2 I_1^{WH}(y_t, y_W) + 2y_t I_2^{WH}(y_t, y_W) \right) \\
&\quad - 8x_b y_t^2 (\zeta_{ts}^{u*} \zeta_{td}^d) (\zeta_{ts}^{d*} \zeta_{td}^u) I_2^{HH}(y_t), \\
C_{H^\pm 1}^{SLL} &= -4x_b y_t^2 (\zeta_{ts}^{d*} \zeta_{td}^u)^2 I_2^{HH}(y_t), \\
C_{H^\pm 1}^{SRR} &= -4x_b y_t^2 (\zeta_{ts}^{u*} \zeta_{td}^d)^2 I_2^{HH}(y_t), \tag{III.5}
\end{aligned}$$

where the subscript H^\pm denotes the charged-Higgs contributions, $y_q = m_q^2/m_{H^\pm}^2$, and the loop integral functions are defined as:

$$I_1^{WH}(y_t, y_W) = \frac{1}{(y_t - y_W)^2} \left[\frac{y_t - y_W}{1 - y_t} + \frac{y_W \ln y_W}{1 - y_W} + \frac{(y_t^2 - y_W) \ln y_t}{(1 - y_t)^2} \right], \tag{III.6a}$$

$$\begin{aligned}
I_2^{WH}(y_t, y_W) &= -\frac{y_t}{2(1 - y_t)(y_t - y_W)} - \frac{y_W^2 \ln y_W}{2(1 - y_W)(y_t - y_W)^2} \\
&\quad - \frac{y_t (y_t + (2 - y_t)y_W) \ln y_t}{2(1 - y_t)^2 (y_t - y_W)^2}, \tag{III.6b}
\end{aligned}$$

$$I_1^{HH}(y_t) = \frac{1 + y_t}{2(1 - y_t)^2} + \frac{y_t \ln y_t}{(1 - y_t)^3}, \tag{III.6c}$$

$$I_2^{HH}(y_t) = -\frac{2}{(1 - y_t)^2} - \frac{(1 + y_t) \ln y_t}{(1 - y_t)^3}. \tag{III.6d}$$

We note through box diagrams that the couplings of $sbH(A)$ and $dbH(A)$ can induce $\Delta S = 2$; however, because the involved quark in the loop is the bottom-quark, the effects should be much smaller than those from the top-quark loop. Here, we ignore their contributions.

To obtain ΔM_K and ϵ_K , we define the hadronic matrix element of $\bar{K}-K$ mixing to be:

$$M_{12}^* = \langle \bar{K}^0 | \mathcal{H}^{\Delta S=2} | K^0 \rangle. \tag{III.7}$$

Accordingly, the K -meson mixing parameter and indirect CP violating parameter can be obtained as:

$$\Delta M_K \approx 2 \text{Re} M_{12}, \quad \epsilon_K \approx \frac{e^{i\pi/4}}{\sqrt{2} \Delta M_K} \text{Im} M_{12}, \tag{III.8}$$

where we have ignored the small contribution of $\text{Im} A_0 / \text{Re} A_0$ from $K \rightarrow \pi\pi$ in ϵ_K . Since ΔM_K is experimentally measured well, we will directly take the ΔM_K data for the denominator of ϵ_K . It has been found that the short-distance SM result on ΔM_K can explain

the data by $\sim 70\%$, and the long-distance effects may contribute another $20 - 30\%$ with a large degree of uncertainty [73]. In this work, we take ΔM_K^{exp} as an input to bound the new physics effects; using the constrained parameters, we then study the implications on the other phenomena.

To estimate the M_{12} defined in Eq. (III.7), we need to run the Wilson coefficients from a higher scale to a lower scale using the renormalization group (RG) equation. In addition, we also need the hadronic matrix elements of $\langle \bar{K}^0 | Q_i | K^0 \rangle$. In order to obtain this information, we adopt the results shown in [69], where the RG and nonperturbative QCD effects have been included. Accordingly, the $\Delta S = 2$ matrix element can be expressed as:

$$\begin{aligned} \langle \bar{K}^0 | \mathcal{H}^{\Delta S=2} | K^0 \rangle = & \frac{G_F^2 V_{\text{CKM}}}{48\pi^2} m_W^2 m_K f_K^2 \{ P_1^{VLL} [C_{F1}^{VLL}(\mu_t) + C_{F1}^{VRR}(\mu_t)] \\ & + P_1^{LR} C_{F1}^{LR}(\mu_t) + P_2^{LR} C_{F2}^{LR}(\mu_t) + P_1^{SLL} [C_{F1}^{SLL}(\mu_t) + C_{F1}^{SRR}(\mu_t)] \\ & + P_2^{SLL} [C_{F2}^{SLL}(\mu_t) + C_{F2}^{SRR}(\mu_t)] \} , \end{aligned} \quad (\text{III.9})$$

where the Wilson coefficients $C_{F_i}^X$ are taken at the m_t scale with $F = S(H^\pm)$, and the values of P_i^X at $\mu = 2$ GeV are [69]:

$$\begin{aligned} P_1^{VLL} &\approx 0.48, & P_1^{LR} &\approx -36.1, & P_2^{LR} &\approx 59.3, \\ P_1^{SLL} &\approx -18.1, & P_2^{SLL} &\approx 32.2. \end{aligned} \quad (\text{III.10})$$

It can be seen that the values of P_i^X , which are related to the scalar operators, are one to two orders of magnitude larger than the value of P_1^{VLL} , where the enhancement factor is from the factor $m_K^2/(m_s + m_d)^2$. The similar enhancement factor in the B -meson system is just slightly larger than one. Although the new physics scale is dictated by $\mu_{S(H^\pm)}$ ($\mu_{S(H^\pm)} > m_t$), as indicated in [69], the RG running of the Wilson coefficients from $\mu_{S(H^\pm)}$ to m_t is necessary only when $\mu_{S(H^\pm)} > 4m_t$. To estimate the new physics effects, we will take $\mu_{S(H^\pm)} \lesssim 800$ GeV and ignore the running effect between $\mu_{S(H^\pm)}$ and m_t scale. In Eq. (III.9), we have explicitly shown the CKM factor to be $V_{\text{CKM}} = 1$ for $F = S$ and $V_{\text{CKM}} = (V_{ts}^* V_{td})^2$ for $F = H^\pm$.

B. $Re(\epsilon'_K/\epsilon_K)$ from the charged-Higgs induced QCD and electroweak penguins

Using isospin decomposition, the decay amplitudes for $K \rightarrow \pi\pi$ can be written as [70]:

$$\begin{aligned} A(K^+ \rightarrow \pi^+\pi^0) &= \frac{3}{2}A_2e^{i\delta_2}, \\ A(K^0 \rightarrow \pi^+\pi^-) &= A_0e^{i\delta_0} + \sqrt{\frac{1}{2}}A_2e^{i\delta_2}, \\ A(K^0 \rightarrow \pi^0\pi^0) &= A_0e^{i\delta_0} - \sqrt{2}A_2e^{i\delta_2} \end{aligned} \quad (\text{III.11})$$

where $A_{0(2)}$ denotes the isospin $I = 0(2)$ amplitude; $\delta_{0(2)}$ is the strong phase, and the measurement is $\delta_0 - \delta_2 = (47.5 \pm 0.9)^\circ$ [70]. In terms of the isospin amplitudes, the direct CP violating parameter in K system can be written as [14]:

$$Re\left(\frac{\epsilon'_K}{\epsilon_K}\right) = -\frac{a\omega}{\sqrt{2}|\epsilon_K|} \left[\frac{ImA_0}{ReA_0}(1 - \hat{\Omega}_{\text{eff}}) - \frac{1}{a} \frac{ImA_2}{ReA_2} \right], \quad (\text{III.12})$$

where $a = 1.017$ [71] and $\hat{\Omega}_{\text{eff}} = (14.8 \pm 8.0) \times 10^{-2}$ [14] include the isospin breaking corrections and the correction of $\Delta I = 5/2$, and

$$\omega = \frac{ReA_2}{ReA_0} \approx \frac{1}{22.46}. \quad (\text{III.13})$$

With the normalizations of $A_{0,2}$ used in [14], the experimental values of ReA_0 and ReA_2 should be taken as:

$$(ReA_0)^{\text{exp}} = 33.22(1) \times 10^{-8} \text{ GeV}, \quad (ReA_2)^{\text{exp}} = 1.479(3) \times 10^{-8} \text{ GeV}. \quad (\text{III.14})$$

Although the uncertainty of the predicted ReA_0 in the SM is somewhat large, the results of ReA_2 obtained by the dual QCD approach [73] and the RBC-UKQCD collaboration [5–7] were consistent with the experimental measurement. Thus, we can use the $(ReA_2)^{\text{exp}}$ to limit the new physics effects. Then, the explanation of the measured $Re(\epsilon'_K/\epsilon_K)$ will rely on the new physics effects that contributes to ImA_0 and ImA_2 .

From Eq. (II.7), the couplings $qqH(A)$ with Cheng-Sher ansatz indeed are suppressed by $m_{d(u)} \tan\beta/v \sim 10^{-3}(\tan\beta/50)$. If we take $m_{H(A)}$ to be heavier, the effects will be further suppressed. Thus, in the following analysis, we neglect the neutral scalar boson contributions to the $K \rightarrow \pi\pi$ processes. According to the results in [58], the couplings $ud(s)H^\pm$ as compared with the SM are small; therefore, we also drop the tree-level charged-Higgs contributions to $K \rightarrow \pi\pi$. Accordingly, the main contributions to the ϵ'_K are from the

top-quark loop QCD and electroweak penguins. Since the induced operators are similar to the SM, in order to consider the RG running of the Wilson coefficients, we thus write the effective Hamiltonian for $\Delta S = 1$ in the form of the SM as [79]:

$$\mathcal{H}^{\Delta S=1} = \frac{G_F}{\sqrt{2}} V_{us}^* V_{ud} \sum_{i=1}^{10} [z_i(\mu) + \tau y_i(\mu)] Q_i(\mu), \quad (\text{III.15})$$

where $\tau = -V_{ts}^* V_{td}/(V_{us}^* V_{ud})$, and $z_i(\mu)$ and $y_i(\mu)$ are the Wilson coefficients at the μ scale. The effective operators for $(V - A) \otimes (V - A)$ are given as:

$$Q_1 = (\bar{s}^\alpha u^\beta)_{V-A} (\bar{u}^\beta d^\alpha)_{V-A}, \quad Q_2 = (\bar{s}u)_{V-A} (\bar{u}d)_{V-A}, \quad (\text{III.16})$$

where α, β are color indices; the color indices in $\bar{q}q'$ are suppressed, and $(\bar{q}q')_{V\pm A} = \bar{q}\gamma_\mu(1 \pm \gamma_5)q'$. For the QCD penguin operators, they are:

$$\begin{aligned} Q_3 &= (\bar{s}d)_{V-A} \sum_q (\bar{q}q)_{V-A}, \quad Q_4 = (\bar{s}^\alpha d^\beta)_{V-A} \sum_q (\bar{q}^\beta q^\alpha)_{V-A}, \\ Q_5 &= (\bar{s}d)_{V-A} \sum_q (\bar{q}q)_{V+A}, \quad Q_6 = (\bar{s}^\alpha d^\beta)_{V-A} \sum_q (\bar{q}^\beta q^\alpha)_{V+A}, \end{aligned} \quad (\text{III.17})$$

where q in the sum includes $u, d, s, c,$ and b quarks. For the electroweak penguins, the effective operators are:

$$\begin{aligned} Q_7 &= \frac{3}{2} (\bar{s}d)_{V-A} \sum_q e_q (\bar{q}q)_{V+A}, \quad Q_8 = \frac{3}{2} (\bar{s}^\alpha d^\beta)_{V-A} \sum_q e_q (\bar{q}^\beta q^\alpha)_{V+A}, \\ Q_9 &= \frac{3}{2} (\bar{s}d)_{V-A} \sum_q e_q (\bar{q}q)_{V-A}, \quad Q_{10} = \frac{3}{2} (\bar{s}^\alpha d^\beta)_{V-A} \sum_q e_q (\bar{q}^\beta q^\alpha)_{V-A}, \end{aligned} \quad (\text{III.18})$$

where e_q is the q -quark electric charge. The H^\pm -mediated Wilson coefficients can be expressed as [79]:

$$\begin{aligned} y_3^{H^\pm}(\mu_H) &= -\frac{\alpha_s(\mu_H)}{24\pi} E_H(y_t) + \frac{\alpha C_H(x_t, y_t)}{6\pi \sin^2 \theta_W}, \quad y_4^{H^\pm}(\mu_H) = \frac{\alpha_s(\mu_H)}{8\pi} E_H(y_t), \\ y_5^{H^\pm}(\mu_H) &= -\frac{\alpha_s(\mu_H)}{24\pi} E_H(y_t), \quad y_6^{H^\pm}(\mu_H) = \frac{\alpha_s(\mu_H)}{8\pi} E_H(y_t), \\ y_7^{H^\pm}(\mu_H) &= \frac{\alpha}{6\pi} (4C_H(x_t, y_t) + D_H(y_t)), \quad y_9^{H^\pm}(\mu_H) = y_7^{H^\pm}(\mu_H) - \frac{4\alpha C_H(x_t, y_t)}{6\pi \sin^2 \theta_W}, \end{aligned} \quad (\text{III.19})$$

$y_8(\mu_H) = y_{10}(\mu_H) = 0$, and the functions $D_H, C_H,$ and E_H are given by [74, 75]:

$$\begin{aligned} C_H(x, y) &= \zeta_{ts}^{u*} \zeta_{td}^u \left[\frac{xy}{8(y-1)} - \frac{xy \ln y}{8(y-1)^2} \right], \\ D_H(y) &= \zeta_{ts}^{u*} \zeta_{td}^u \frac{y}{3} \left[\frac{47y^2 - 79y + 38}{36(y-1)^3} + \frac{-3y^3 + 6y - 4}{6(y-1)^4} \ln y \right], \\ E_H(y) &= \zeta_{ts}^{u*} \zeta_{td}^u \left[\frac{y(7y^2 - 29y + 16)}{36(y-1)^3} + \frac{y(3y-2)}{6(y-1)^4} \ln y \right]. \end{aligned} \quad (\text{III.20})$$

To calculate ϵ'_K , in addition to the Wilson coefficients, we need the hadronic matrix elements of the effective operators. The $Q_{1,2}$ matrix elements can be obtained from ReA_0 and ReA_2 through the parametrizations [14]:

$$\begin{aligned}
ReA_0 &\approx \frac{G_F}{\sqrt{2}} V_{us}^* V_{ud} (z_+ \langle Q_+ \rangle_0 + z_- \langle Q_- \rangle_0) \\
&= \frac{G_F}{\sqrt{2}} V_{us}^* V_{ud} (1+q) z_- \langle Q_- \rangle_0, \\
ReA_2 &\approx \frac{G_F}{\sqrt{2}} V_{us}^* V_{ud} z_+ \langle Q_+ \rangle_2,
\end{aligned} \tag{III.21}$$

where we ignore the small imaginary part in $V_{us}^* V_{ud}$; the Wilson coefficients and the matrix elements of the effective operators are taken at the $\mu = m_c$ scale; the subscripts of the brackets denote the isospin states $I = 0$ and $I = 2$; $z_{\pm} = z_2 \pm z_1$, $Q_{\pm} = (Q_2 \pm Q_1)/2$, $z_1(m_c) = -0.4092$, $z_2(m_c) = 1.2120$, and $q = z_+ \langle Q_+ \rangle_0 / (z_- \langle Q_- \rangle_0)$. In the isospin limit, the hadronic matrix elements of $Q_{4,9,10}$ can be related to $Q_{+,-}$ [72]. Therefore, we show the matrix elements for isospin $I = 0$ as [14, 72]:

$$\begin{aligned}
\langle Q_4 \rangle_0 &= 2 \langle Q_- \rangle_0, \quad \langle Q_9 \rangle_0 = \frac{3}{2} (\langle Q_+ \rangle_0 - \langle Q_- \rangle_0), \\
\langle Q_{10} \rangle_0 &= \frac{3}{2} \langle Q_+ \rangle_0 + \frac{1}{2} \langle Q_- \rangle_0, \\
\langle Q_6 \rangle_0 &= -4h \left(\frac{m_K^2}{m_s(m_c) + m_d(m_c)} \right)^2 (f_K - f_\pi) B_6^{(1/2)}, \\
\langle Q_8 \rangle_0 &= 2h \left(\frac{m_K^2}{m_s(m_c) + m_d(m_c)} \right)^2 f_\pi B_8^{(1/2)},
\end{aligned} \tag{III.22}$$

for isospin $I = 2$, they are given as:

$$\begin{aligned}
\langle Q_9 \rangle_2 &= \langle Q_{10} \rangle_2 = \frac{3}{2} \langle Q_+ \rangle_2, \\
\langle Q_8 \rangle_2 &= \sqrt{2} h \left(\frac{m_K^2}{m_s(m_c) + m_d(m_c)} \right)^2 f_\pi B_8^{(3/2)},
\end{aligned} \tag{III.23}$$

where $h = \sqrt{3/2}$; the small matrix elements for $Q_{3,5,7}$ are neglected; $B_6^{(1/2)} = 0.57 \pm 0.19$, $B_8^{(3/2)} = 0.76 \pm 0.05$, and $B_8^{(1/2)} = 1.0 \pm 0.2$ [23], which are extracted from the lattice calculations [8, 9].

Using the introduced hadronic matrix elements and Eq. (III.12), the direct CP violating

parameter via the charged-Higgs contributions can be expressed as:

$$\text{Re} \left(\frac{\epsilon'_K}{\epsilon_K} \right)_{H^\pm} = \text{Im} \left[\lambda_t \left(a(1 - \hat{\Omega}_{\text{eff}}) P_{H^\pm}^{(1/2)} - P_{H^\pm}^{(3/2)} \right) \right], \quad (\text{III.24a})$$

$$P_{H^\pm}^{(1/2)} = a_0^{(1/2)}(H^\pm) + a_6^{(1/2)}(H^\pm) B_6^{(1/2)}, \quad (\text{III.24b})$$

$$P_{H^\pm}^{(3/2)} = a_0^{(3/2)}(H^\pm) + a_8^{(3/2)}(H^\pm) B_8^{(3/2)}, \quad (\text{III.24c})$$

where $\lambda_t = V_{ts}^* V_{td}$, $a_i^{\Delta I}$ are defined as [14]:

$$\begin{aligned} a_0^{(1/2)}(H^\pm) &\approx r_1 \frac{4y_4^{H^\pm} - b(3y_9^{H^\pm} - y_{10}^{H^\pm})}{2(1+q)z_-} + r_2 b y_8^{H^\pm} \frac{\langle Q_8 \rangle_0}{\text{Re} A_0}, \\ a_6^{(1/2)}(H^\pm) &\approx r_2 y_6^{H^\pm} \frac{\langle Q_6 \rangle_0}{B_6^{(1/2)} \text{Re} A_0}, \\ a_0^{(3/2)}(H^\pm) &\approx r_1 \frac{3(y_9^{H^\pm} + y_{10}^{H^\pm})}{2z_+}, \\ a_8^{(3/2)}(H^\pm) &\approx r_2 y_8^{H^\pm} \frac{\langle Q_8 \rangle_2}{B_8^{(3/2)} \text{Re} A_2}, \end{aligned} \quad (\text{III.25})$$

with $b = 1/(a(1 - \hat{\Omega}_{\text{eff}}))$,

$$r_1 = \frac{\omega}{\sqrt{2}|\epsilon_K|V_{us}^*V_{ud}} \approx 64.545, \quad r_2 = \frac{\omega G_F}{2|\epsilon_K|} \approx 1.165 \times 10^{-4} \text{ GeV}^{-2}. \quad (\text{III.26})$$

We note that the Wilson coefficients in Eq. (III.25) should be taken at the $\mu = m_c$ scale through the RG running.

IV. CHARGED-HIGGS ON THE $K \rightarrow \pi \nu \bar{\nu}$ DECAYS

To investigate the new physics contributions to the rare K decays, we adopt the parametrizations shown in [24] as:

$$\text{BR}(K^+ \rightarrow \pi^+ \bar{\nu} \nu) = \kappa_+(1 + \Delta_{EM}) \left[\left(\frac{\text{Im} X_{\text{eff}}}{\lambda^5} \right)^2 + \left(\frac{\text{Re} \lambda_c}{\lambda} P_c(X) + \frac{\text{Re} X_{\text{eff}}}{\lambda^5} \right)^2 \right], \quad (\text{IV.1})$$

$$\text{BR}(K_L \rightarrow \pi^0 \bar{\nu} \nu) = \kappa_L \left(\frac{\text{Im} X_{\text{eff}}}{\lambda^5} \right)^2, \quad (\text{IV.2})$$

where λ is the Wolfenstein parameter; $\Delta_{EM} = -0.003$; $P_c(X) = 0.404 \pm 0.024$ denotes the charm-quark contribution [23, 76, 77]; $X_{\text{eff}} = V_{ts}^* V_{td} [X_L^{\text{SM}}(K) + X_L(K) + X_R(K)]$ combines the new physics contributions and the SM result of $X_L^{\text{SM}}(K) = 1.481 \pm 0.009$ [24], and the

values of $\kappa_{+,L}$ are given as:

$$\begin{aligned}\kappa_+ &= (5.173 \pm 0.025) \times 10^{-11} \left(\frac{\lambda}{0.225} \right)^8, \\ \kappa_L &= (2.231 \pm 0.013) \times 10^{-10} \left(\frac{\lambda}{0.225} \right)^8.\end{aligned}\tag{IV.3}$$

Here, $X_L(K)$ and $X_R(K)$ denote the contributions from the left-handed and right-handed quark currents, respectively.

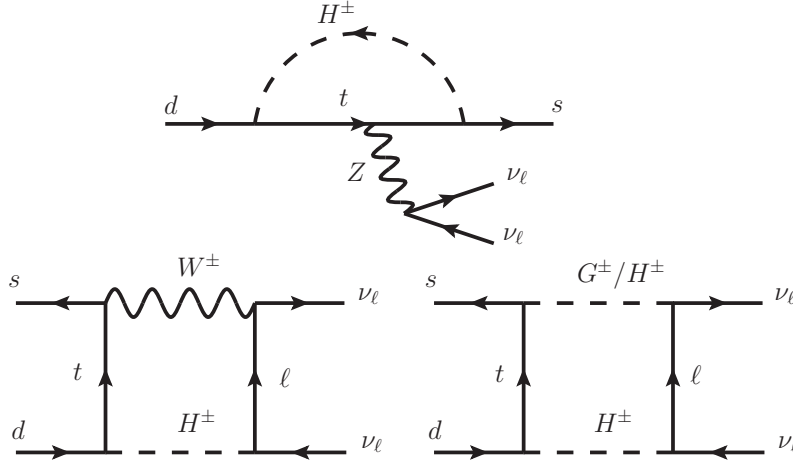


FIG. 2: Sketched Feynman diagrams for the $K \rightarrow \pi \bar{\nu} \nu$ process.

The neutral scalar bosons H and A do not couple to neutrinos; therefore, the rare $K \rightarrow \pi \nu \bar{\nu}$ decays can be generated by the Z -mediated electroweak penguins and the W^\pm - and H^\pm -mediated box diagrams, for which the representative Feynman diagrams are shown in Fig. 2. Since the dominant H^\pm contributions are from the left-handed quark currents, we only show the $X_L(K)$ results in the following analysis. Using the H^\pm Yukawa couplings in Eq. (II.11), the Z -penguin contribution can be obtained as:

$$\begin{aligned}X_{L,\text{Pen}}^{H^\pm} &= g_L^u \zeta_{ts}^{u*} \zeta_{td}^u x_t y_t J_1(y_t), \\ J_1(y_t) &= -\frac{1}{4} \left(\frac{1}{1-y_t} + \frac{\ln y_t}{(1-y_t)^2} \right),\end{aligned}\tag{IV.4}$$

where g_L^u is the Z -boson coupling to the left-handed up-type quarks and is given as $g_L^u = 1/2 - 2 \sin^2 \theta_W / 3$ with $\sin^2 \theta_W \approx 0.23$, and $J_1(y_t)$ is the loop integral function.

According to the intermediated states in the loops, there are three types of box diagrams contributing to the $d \rightarrow s \nu \bar{\nu}$ process: $W^\pm H^\pm$, $G^\pm H^\pm$, and $H^\pm H^\pm$. Their results are

respectively shown as follows. For the $W^\pm H^\pm$ diagrams, the result is obtained as:

$$X_{L,\text{Box}}^{W^\pm H^\pm, \ell} = -\frac{1}{\sqrt{3}}(\zeta_{td}^u \zeta_\ell^\ell + \zeta_{ts}^{u*} \zeta_\ell^{\ell*}) x_\ell y_t t_\beta J_2(y_t, y_W), \quad (\text{IV.5})$$

$$J_2(y_t, y_W) = I_2(y_t, y_W) - I_2(y_t, 0),$$

$$I_2(y_t, y_W) = -\frac{1}{4(y_t - y_W)} \left[\frac{2 - y_t}{1 - y_t} \ln y_t - \frac{y_W}{1 - y_W} \ln y_W \right]. \quad (\text{IV.6})$$

where $x_\ell = m_\ell^2/m_W^2$, and the function J_2 is the loop integration. The result of $G^\pm H^\pm$ diagrams is given as:

$$X_{L,\text{Box}}^{G^\pm H^\pm, \ell} = \frac{1}{\sqrt{3}}(\zeta_{td}^u \zeta_\ell^\ell + \zeta_{ts}^{u*} \zeta_\ell^{\ell*}) x_\ell y_t t_\beta J_3(y_t, y_W), \quad (\text{IV.7})$$

$$J_3(y_t, y_W) = \frac{1}{8} \int_0^1 dx_1 \int_0^{x_1} dx_2 \int_0^{x_2} dx_3 \frac{1}{1 - (1 - y_t)x_1 - (y_t - y_W)x_2 - y_W x_3}.$$

It can be seen that except the loop functions, $X_{L,\text{Box}}^{G^\pm H^\pm}$ and $X_{L,\text{Box}}^{W^\pm H^\pm}$ have the common factor from the charged-Higgs effect. The pure H^\pm -loop contribution to the box diagram can be written as:

$$X_{L,\text{Box}}^{H^\pm H^\pm, \ell} = -\frac{1}{\sqrt{3}} \zeta_{ts}^{u*} \zeta_{td}^u |\zeta_\ell^\ell|^2 x_\ell y_t \tan^2 \beta J_4(y_t),$$

$$J_4(y_t) = \frac{1}{48} \left[\frac{1}{1 - y_t} + \frac{y_t \ln y_t}{(1 - y_t)^2} \right]. \quad (\text{IV.8})$$

Because the lepton Yukawa coupling is proportional to the lepton mass, all of the box diagrams depend on $x_\ell = m_\ell^2/m_W^2$; therefore, they are dominated by the τ -lepton. Although the $W^\pm H^\pm$ and $G^\pm H^\pm$ diagrams have a $\tan \beta$ enhancement, the enhancement factor of $H^\pm H^\pm$ is $\tan^2 \beta$; that is, the $H^\pm H^\pm$ contribution overwhelms the $W^\pm H^\pm$ and $G^\pm H^\pm$.

V. NUMERICAL ANALYSIS

A. Numerical inputs

The new free parameters considered in this study are $\chi_{tt,ct}^u$, $\chi_{bb,bs,bd}^d$, χ_τ^ℓ , t_β , and m_{H,A,H^\pm} . In addition to ΔM_K and ϵ_K , the charged-Higgs related parameters also contribute to the $\Delta M_{B_{d(s)}}$ and $B \rightarrow X_s \gamma$ processes, so we have taken these observables into account to constrain the parameters. Thus, the experimental data used to bound the free parameters

are [68]:

$$\begin{aligned}
\Delta M_K^{\text{exp}} &\approx 3.48 \times 10^{-15} \text{ GeV}, \quad \Delta M_{B_d}^{\text{exp}} = (3.332 \pm 0.0125) \times 10^{-13} \text{ GeV} \\
\Delta M_{B_s}^{\text{exp}} &= (1.168 \pm 0.014) \times 10^{-11} \text{ GeV}, \quad BR(B \rightarrow X_s \gamma)^{\text{exp}} = (3.49 \pm 0.19) \times 10^{-4}, \\
\epsilon_K^{\text{exp}} &\approx 2.228 \times 10^{-3}.
\end{aligned} \tag{V.1}$$

Since ϵ_K in the SM fits well with the experimental data [79], we use

$$\epsilon_K^{\text{NP}} = \kappa_\epsilon \times 10^{-3} \text{ with } |\kappa_\epsilon| < 0.4 \tag{V.2}$$

to constrain the new physics effects [26]. The uncertainties of NLO [82] and NNLO [83] QCD corrections to the short-distance contribution to ΔM_K in the SM are somewhat large, we take the combination of the short-distance (SD) and long-distance (LD) effects as $\Delta M_K^{\text{SM}}(SD + LD) = (0.80 \pm 0.10)\Delta M_K^{\text{exp}}$ [73]. Accordingly, the new physics contribution to ΔM_K is limited to:

$$\Delta M_K^{\text{NP}} = r_K \Delta M_K^{\text{exp}} \text{ with } |r_K| < 0.2. \tag{V.3}$$

Although the charged-Higgs can generally contribute to the tree-level processes and contaminate the determination of CKM matrix elements, the charged-Higgs-induced tree processes indeed can be ignored because these processes, which can determine $V_{ud,cs}$, $V_{ud,cd}$, and $V_{ub,cb}$, will be suppressed by $1 - \chi_\ell^\ell/s_\beta$ when $\chi_\ell^\ell \sim 1$ are taken. Then, the CKM matrix elements mentioned above can be taken the same as those obtained in the SM. With the Wolfenstein parametrization [84], the CKM matrix elements can be taken as:

$$\begin{aligned}
V_{ud} &\approx V_{cs} \approx 1 - \lambda^2/2, \quad V_{us} \approx -V_{cd} \approx \lambda = 0.225, \\
V_{cb} &\approx 0.0407, \quad V_{ub} \approx 0.0038e^{-i\phi_3}, \quad \phi_3 = 73.5^\circ,
\end{aligned} \tag{V.4}$$

where V_{cb} and V_{ub} are taken from the averages of inclusive and exclusive semileptonic decays [23], and the ϕ_3 angle is the central value averaged by the heavy flavor averaging group (HFLAV) through all charmful two-body B -meson decays [85]. In terms of the CKM matrix elements shown in Eq. (V.4), we can obtain the other CKM matrix elements and CP phase of V_{td} as [23]:

$$\begin{aligned}
R_b &\approx \left(1 - \frac{\lambda^2}{2}\right) \frac{|V_{ub}|}{\lambda|V_{cb}|} \approx 0.40, \\
R_t &= (1 + R_b^2 - 2R_b \cos \phi_3)^{1/2} \approx 0.96, \quad V_{ts} \approx -V_{cb}, \quad V_{tb} \approx 1, \\
|V_{td}| &= |V_{us}||V_{cb}|R_t \approx 0.0088, \quad \phi_2 = \arccot\left(\frac{1 - R_b \cos \phi_3}{R_b \sin \phi_3}\right) \approx 23.4^\circ,
\end{aligned} \tag{V.5}$$

where $Re(V_{ts}^*V_{td}) \approx -3.3 \times 10^{-4}$ and $Im(V_{ts}^*V_{td}) \approx 1.4 \times 10^{-4}$ are close to those values used in [14].

The particle masses used to estimate the numerical values are given as:

$$\begin{aligned} m_K &\approx 0.489 \text{ GeV}, \quad m_{B_d} \approx 5.28 \text{ GeV}, \quad m_{B_s} \approx 5.37 \text{ GeV}, \quad m_W \approx 80.385 \text{ GeV}, \\ m_t &\approx 165 \text{ GeV}, \quad m_c \approx 1.3 \text{ GeV}, \quad m_s(m_c) \approx 0.109 \text{ GeV}, \quad m_d(m_c) \approx 5.44 \text{ MeV}. \end{aligned} \quad (\text{V.6})$$

In the 2HDM, the mass spectra of H , A and H^\pm are not independent parameters, and they are correlated through the parameters in the Higgs potential and constrained by the vacuum stability, Peskin-Takeuchi parameters [86], and Higgs precision measurements [87]. Following the results in [87], the maximum mass difference $|m_{H(A)} - m_{H^\pm}|$ should be around 100 GeV when $m_H = m_A$ is adopted. Since the interesting region of m_{H^\pm} in this study is near 200 GeV, we take $m_{H(A)} = 300 \text{ GeV}$ as the input to show the numerical analysis.

B. Direct bound on m_{H^\pm} from the LHC

According to Eq. (II.13), if we take $\chi_\tau^\ell = 1$, the H^\pm Yukawa coupling to the tau-lepton is suppressed by $1 - \chi_\tau^\ell/s_\beta$; therefore, in our case, the charged-Higgs with $m_{H^\pm} \sim 200 \text{ GeV}$ predominantly decays to the $t\bar{b}$ final state. Thus, the experimental limit on m_{H^\pm} is from the CMS data at $\sqrt{s} = 8 \text{ TeV}$ [88], and the upper bound for $m_{H^\pm} = 200 \text{ GeV}$ and $BR(H^+ \rightarrow t\bar{b}) = 1$ is $\sigma(pp \rightarrow \bar{t}(b)H^\pm) < 1.53 \text{ pb}$ [89], where the cross section $\sigma(pp \rightarrow \bar{t}(b)H^\pm)$ includes the $pp \rightarrow \bar{t}(b)H^+$ and $pp \rightarrow t(\bar{b})H^-$ contributions. From the Yukawa sector, the tbH^\pm couplings can be expressed as:

$$\begin{aligned} \mathcal{L}_Y^{H^\pm} &\supset \frac{\sqrt{2}}{v} V_{tb} \bar{t} (m_t \zeta_{tb}^u P_L + m_b \zeta_{tb}^d P_R) b + H.c., \\ \zeta_{tb}^u &= \frac{1}{t_\beta} - \frac{\chi_{tt}^{u*}}{s_\beta}, \quad \zeta_{tb}^d = t_\beta \left(1 - \frac{\chi_{bb}^d}{s_\beta} \right). \end{aligned} \quad (\text{V.7})$$

Accordingly, the main charged-Higgs production channel is $gg \rightarrow \bar{t}bH^+$ in four-flavor scheme (4FS) and is $g\bar{b} \rightarrow \bar{t}H^+$ in five-flavor scheme (5FS), where the 4FS and 5FS are used to avoid double counting, which happens when the b -quark final state in $gg \rightarrow \bar{t}bH^+$ escapes detection [90–92].

To estimate the production cross-section for $pp \rightarrow \bar{t}(b)H^\pm$, we employ CalcHEP [93] associated with the CTEQ6L parton distribution functions (PDFs) [94]. Using $t_\beta = 30$, $\chi_{bb}^d = 0.5$, and $m_{H^\pm} = 200 \text{ GeV}$, the $\sigma(pp \rightarrow \bar{t}(b)H^\pm)$ at $\sqrt{s} = 8 \text{ TeV}$ as a function of χ_{tt}^u is

shown in Fig. 3(a), where the dashed line is the CMS upper limit, and $K = 1.3$ denotes the K -factor for the radiative QCD corrections [95]. The dependence of $\sigma(pp \rightarrow \bar{t}(b)H^\pm)$ on t_β is shown in Fig. 3(b), where $\chi_{tt}^u = 0.5$, $\chi_{bb}^d = 0.5$, $m_{H^\pm} = 200$ GeV, and $K = 1.3$ are used. From the plots, it can be seen that taking proper values of χ_{tt}^u and χ_{bb}^d , both $m_{H^\pm} \sim 200$ GeV and large t_β value can still satisfy the upper limit from the direct search.

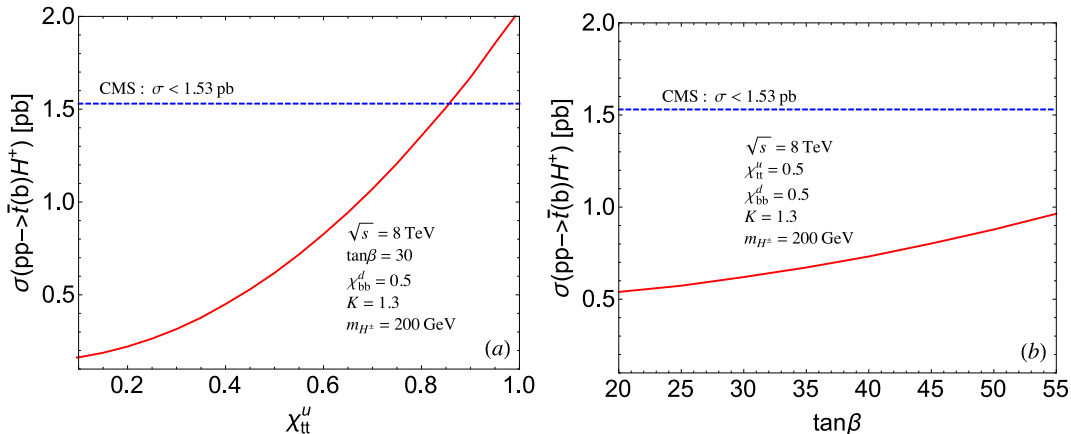


FIG. 3: Production cross-section of $pp \rightarrow \bar{t}(b)H^+$ (solid) at $\sqrt{s} = 8$ TeV as a function of (a) χ_{tt}^u and (b) t_β , where the fixed values of parameters are given in the plots, $K = 1.3$ is the K -factor for the radiative QCD corrections, and the dashed line denotes the CMS upper bound.

C. Constraints from $\Delta M_{K,B}$, $B \rightarrow X_s \gamma$, and ϵ_K

Since the free parameters for the tree-induced $\Delta S = 2$ are different from those that are box-induced, we analyze them separately. According to Eq. (III.4), in addition to the t_β parameter, the main parameters in the H/A -mediated M_{12} are $\chi_{ds}^{d*} \chi_{sd}^d = |\chi_{ds}^{d*} \chi_{sd}^d| e^{-i\theta_{CP}}$, where θ_{CP} is the weak CP-violation phase. Using Eq. (III.9) and the taken input values, ΔM_K (solid) and ϵ_K (dashed) as a function of $|\chi_{ds}^{d*} \chi_{sd}^d|$ (in units of 10^{-4}) and θ_{CP} are shown in Fig. 4, where we only show the range of $\theta_{CP} = [0, \pi]$ and fix $t_\beta = 30$. It is seen that the typical value of $|\chi_{ds}^{d*} \chi_{sd}^d|$ constrained by the $K^0 - \bar{K}^0$ mixing is $\sim 4.5 \times 10^{-3}$. Because the ϵ_K and ΔM_K both arise from the same complex parameter $\chi_{ds}^{d*} \chi_{sd}^d$, to obtain ϵ_K of $O(10^{-3})$, the CP-violation phase θ_{CP} inevitably has to be of $O(10^{-3})$ away from zero or π when the $|\chi_{ds}^{d*} \chi_{sd}^d|$ of $O(10^{-5})$ is taken. Intriguingly, the small θ_{CP} may not be a fine-tuning result in the case of $m_H = m_A$. If the Yukawa matrices Y_i^f in Eq. (II.2) are symmetric matrices, due

to $V_R^f = V_L^{f*}$, \mathbf{X}^f in Eq. (II.4) also being symmetric, we can obtain $\chi_{ds}^d = \chi_{sd}^d$ and $\theta_{CP} = 0$. Hence, a small θ_{CP} can be ascribed to a slight break in a symmetric Yukawa matrix.

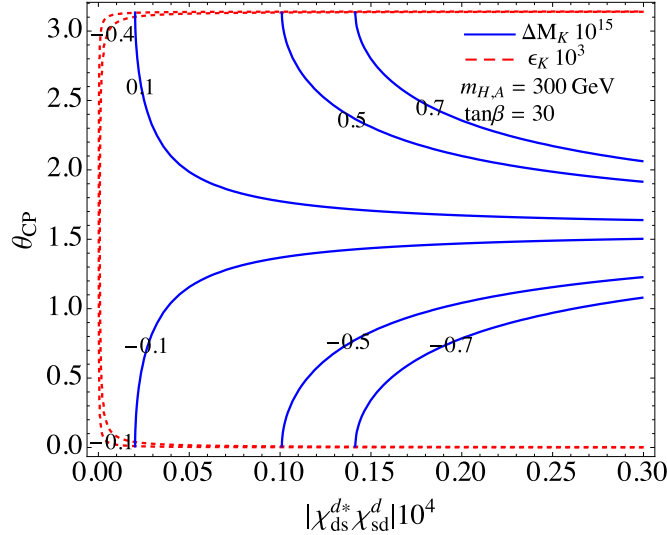


FIG. 4: Contours for the H/A -mediated ΔM_K (in units of 10^{-15}) and ϵ_K (in units of 10^{-3}) as a function of $|\chi_{ds}^{d*}\chi_{sd}^d|$ scaled by 10^{-4} and θ_{CP} .

Next, we analyze the charged-Higgs loop contributions to ΔM_K and ϵ_K . According to Eqs. (II.11) and (II.12), the relevant Yukawa couplings are $\chi_{tt,ct}^u$ and $\chi_{bd,bs}^d$. However, the same parameters also contribute to $\Delta M_{B_{d,s}}$ and $B \rightarrow X_s \gamma$, where the former can arise from the tree H/A -mediated and charged-Higgs-mediated box diagrams, and the latter is from the H^\pm -penguin loop diagrams [58]. Thus, we have to constrain the free parameters by taking the $\Delta M_{B_{d,B_s}}$ and $B \rightarrow X_s \gamma$ data into account. To scan the parameters, we set the ranges of the scanned parameters to be:

$$\begin{aligned}
 -1 \leq \chi_{tt}^u, \chi_{ct}^u, \chi_{bb}^d \leq 1, \quad -0.05 \leq \chi_{bd}^d, \chi_{bs}^d \leq 0.05, \\
 20 \leq t_\beta \leq 50, \quad 200 \leq m_{H^\pm} [\text{GeV}] \leq 230.
 \end{aligned}
 \tag{V.8}$$

ϵ'_K/ϵ_K can be significantly enhanced only by the light H^\pm ; therefore, we set m_{H^\pm} around 200 GeV.

In order to consider the constraints from the B -meson decays, we use the formulae and results obtained in [58]. To understand the influence of B and K systems on the parameters, we show the constraints with and without the ΔM_K and ϵ_K constraints. Thus, for the $\Delta M_{B_{d,B_s}}$ and $B \rightarrow X_s \gamma$ constraints only, we respectively show the allowed ranges of χ_{tt}^u

and χ_{ct}^u and the allowed ranges of χ_{bs}^d and χ_{bd}^d in Fig. 5(a) and (b), where the sampling data points for the scan are $5 \cdot 10^6$. When the ΔM_K and ϵ_K constraints are included, the corresponding situations are shown in Fig. 6(a) and (b), respectively. From the plots, it can be clearly seen that K -meson data can further constrain the free parameters. We note that the results of Fig. 6 do not include the tree-induced $\Delta S = 2$ because the involved parameters are different.

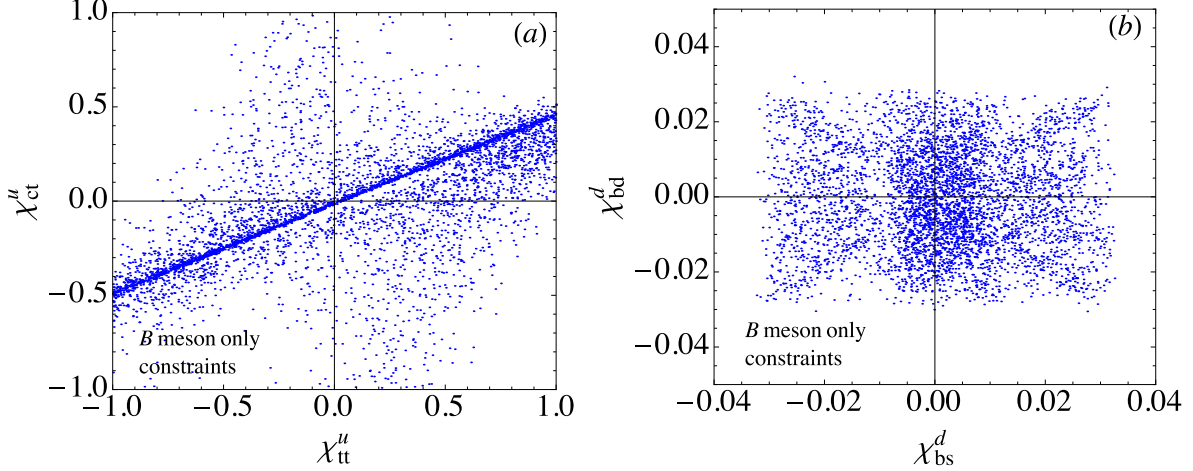


FIG. 5: Constraints from $\Delta M_{B_d, B_s}$ and $B \rightarrow X_s \gamma$, where the plots (a) and (b) denote the allowed ranges of χ_{tt}^u and χ_{ct}^u and the allowed ranges of χ_{bs}^d and χ_{bd}^d , respectively. The number of sample points used for the scan is $5 \cdot 10^6$.

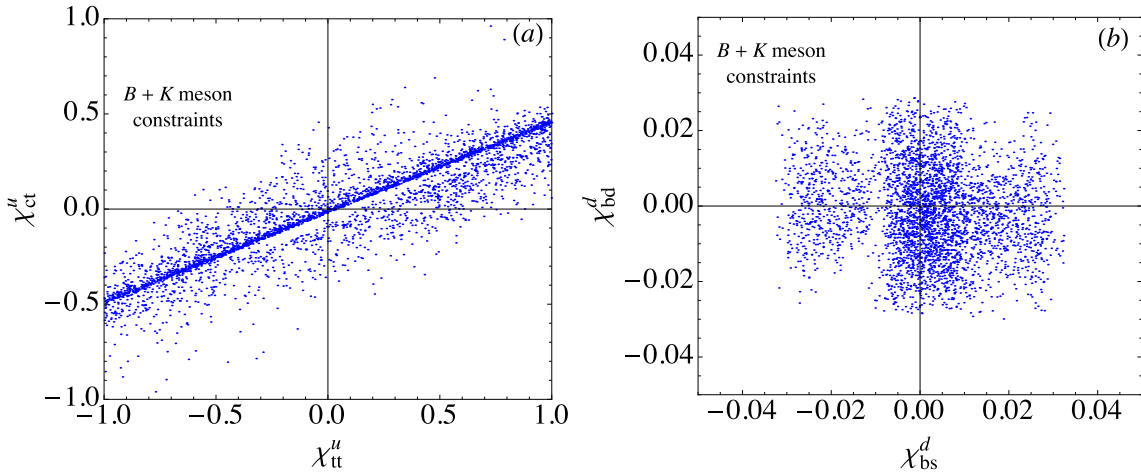


FIG. 6: Based on the results in Fig. 5, the constraints from the H^\pm -induced ΔM_K and ϵ_K are included.

It was studied that the charged-Higgs and neutral Higgs bosons h , H and A can also

have significant contributions to the rare $B_s \rightarrow \mu^+ \mu^-$ decay through loop and tree Feynman diagrams in the type-III 2HDM [96–99] when a large t_β scheme is applied, where the current LHCb measurement is $BR(B_s \rightarrow \mu^+ \mu^-) = (3.0 \pm 0.6_{-0.2}^{+0.3}) \times 10^{-9}$ [100] and the SM prediction is $BR(B_s \rightarrow \mu^+ \mu^-) = (3.65 \pm 0.23) \times 10^{-9}$ [101]. The small difference in $BR(B_s \rightarrow \mu^+ \mu^-)$ between experimental and theoretical result leads to a strict constraint on the new physics contribution. From the Yukawa couplings shown in Eqs. (II.3) and (II.5), it can be seen that under the alignment limit (i.e., $\beta - \alpha = \pi/2$), which we adopt in the paper, H^\pm , H , and A bosons coupling to the leptons are all proportional to $1 - \chi_\mu^\ell/s_\beta$ when the Cheng-Sher ansatz is applied. That is, the contributions to the $B_s \rightarrow \mu^+ \mu^-$ decay, which arise from the H^\pm -induced box diagrams and $H(A)$ -penguin and $H(A)$ -tree diagrams, can be suppressed in the type-III 2HDM when $\chi_\mu^\ell \sim 1$ is taken. The choice of $\chi_\mu^\ell \sim 1$ matches with the condition of $\chi_\ell^\ell \sim 1$ used for taking the SM CKM matrix elements as the numerical inputs. Hence, in this study, we do not include the constraint from the $B_s \rightarrow \mu^+ \mu^-$ decay.

D. $Re(\epsilon'_K/\epsilon_K)$ in the 2HDM

In this subsection, we analyze the charged-Higgs effect on $Re(\epsilon'_K/\epsilon_K)_{H^\pm}$ in detail. To estimate $Re(\epsilon'_K/\epsilon_K)_{H^\pm}$, we need to run the Wilson coefficients from the μ_H scale to the $\mu = m_c$ scale. For new physics effects, we use the LO QCD corrections to the QCD and electroweak penguin operators [79]; as a result, the relevant Wilson coefficients at the $\mu = m_c$ scale can be obtained as:

$$\begin{aligned}
y_4^{H^\pm}(m_c) &\approx -0.6y_3^{H^\pm}(\mu_H) + 1.07y_4^{H^\pm}(\mu_H) + 0.08y_5^{H^\pm}(\mu_H) \\
&\quad + 0.46y_6^{H^\pm}(\mu_H) + 0.016y_7^{H^\pm}(\mu_H) + 0.068y_9^{H^\pm}(\mu_H), \\
y_6^{H^\pm}(m_c) &\approx -0.1y_3^{H^\pm}(\mu_H) + 0.388y_4^{H^\pm}(\mu_H) + 0.794y_5^{H^\pm}(\mu_H) \\
&\quad + 2.872y_6^{H^\pm}(\mu_H) + 0.02y_7^{H^\pm}(\mu_H) + 0.1y_9^{H^\pm}(\mu_H), \\
y_8^{H^\pm}(m_c) &\approx 0.904y_7^{H^\pm}(\mu_H), \quad y_9^{H^\pm}(m_c) \approx 1.31y_9^{H^\pm}(\mu_H), \\
y_{10}^{H^\pm}(m_c) &\approx -0.58y_9^{H^\pm}(\mu_H),
\end{aligned} \tag{V.9}$$

where the Λ scale in α_s is determined by $\alpha_s^{(f=5)}(m_Z) = 0.118$.

According to the parametrization of $Re(\epsilon'_K/\epsilon_K)$ defined in Eq. (III.24), four pieces contribute to the direct CP violation; two of them, $a_0^{(1/2)}(H^\pm)$ and $a_6^{(1/2)}(H^\pm)B_6^{(1/2)}$, are from $P_{H^\pm}^{(1/2)}$, and the other two, $a_0^{(3/2)}(H^\pm)$ and $a_8^{(3/2)}(H^\pm)B_8^{(3/2)}$, are from $P_{H^\pm}^{(3/2)}$. To understand

their contributions to ϵ'_K/ϵ_K , we show each individual effect as a function of χ_{ct}^u in Fig. 7, where for numerical illustration, we have fixed $\chi_{tt}^u = 0.3$, $t_\beta = 30$, and $m_{H^\pm} = 200$ GeV. From the results, it can be seen that $a_8^{3/2} B_8^{3/2}$, which arises from the electroweak penguin Q_8 operator, dominates the others.

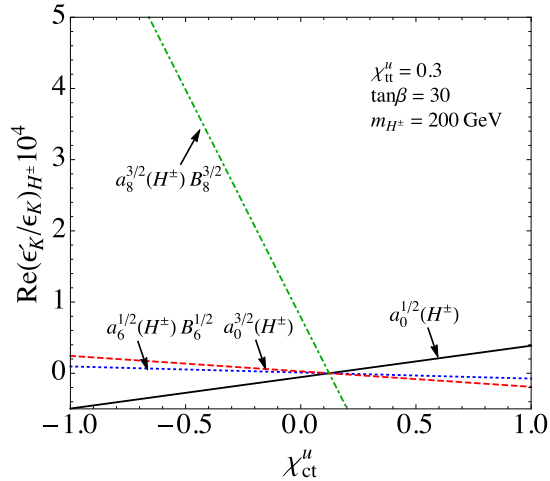


FIG. 7: Each contribution of $a_0^{1/2}(H^\pm)$, $a_6^{1/2}(H^\pm)B_6^{(1/2)}$, $a_0^{3/2}(H^\pm)$, and $a_8^{3/2}(H^\pm)B_8^{3/2}$ defined in Eq. (III.25), where we fixed $\chi_{tt}^u = 0.3$, $t_\beta = 30$, and $m_{H^\pm} = 200$ GeV.

From our analysis, it was found that to enhance $(\epsilon'_K/\epsilon_K)_{H^\pm}$, χ_{tt}^u and χ_{ct}^u prefer to be opposite in sign. In the following numerical analysis, we narrow the scan ranges of χ_{tt}^u and χ_{ct}^u to be:

$$0.4 \leq \chi_{tt}^u \leq 0.8, \quad -0.8 \leq \chi_{ct}^u \leq 0.1. \quad (\text{V.10})$$

In order to include the tree-induced $\Delta S = 2$ effects shown in Eq. (III.3), we set the relevant parameters as:

$$|\chi_{ds}^{d*} \chi_{sd}^d| \leq 0.8 \times 10^{-6}, \quad |\theta_{CP}| \leq \pi. \quad (\text{V.11})$$

Since we now need to combine the H^\pm -induced box diagrams and the $H(A)$ -induced tree diagrams for the $\Delta S = 2$ process, to satisfy the constraints of ΔM_K and ϵ_K and enhance ϵ'_K/ϵ_K , the taken values of $|\chi_{ds}^{d*} \chi_{sd}^d|$ are smaller than those shown in Fig. 4. When the constraints from the B and K systems are taken into account, in which the sampling data points for the scan are $2.5 \cdot 10^7$, the dependence of $Re(\epsilon'_K/\epsilon_K)_{H^\pm}$ (in units of 10^{-4}) on the parameters is given as follows: Fig. 8(a) shows $Re(\epsilon'_K/\epsilon_K)_{H^\pm}$ as a function of m_{H^\pm} ; Fig. 8(b) and (c) are the dependence of χ_{ct}^u and χ_{bs}^d , respectively, and Fig. 8(d) shows the correlation

between $Re(\epsilon'_K/\epsilon_K)_{H^\pm}$ and $\epsilon_K^S + \epsilon_K^{H^\pm}$ (in units of 10^{-3}). Since the dependence of χ_{bd}^d is similar to that of χ_{bs}^d , we do not show the case for χ_{bd}^d . From these plots, we see that although we cannot push $(\epsilon'_K/\epsilon_K)_{H^\pm}$ up to $O(10^{-3})$, the charged-Higgs effects can lead to $(\epsilon'_K/\epsilon_K)_{H^\pm} \sim 8 \times 10^{-4}$.

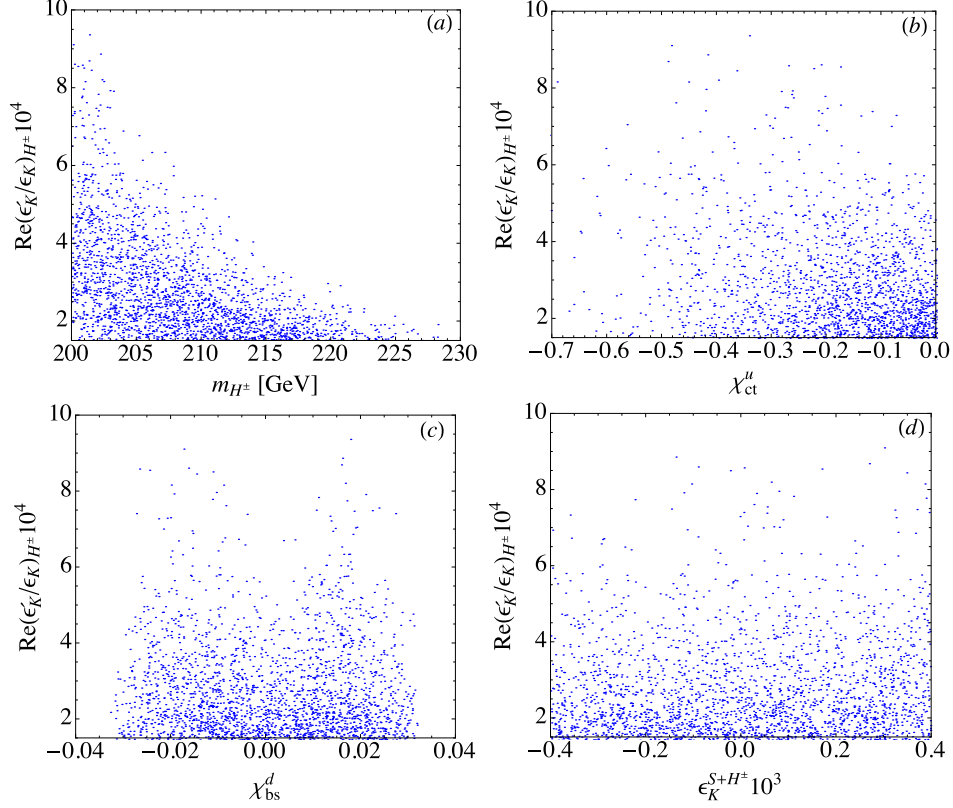


FIG. 8: $Re(\epsilon'_K/\epsilon_K)_{H^\pm}$ (in units of 10^{-4}) as a function of (a) m_{H^\pm} , (b) χ_{ct}^u , and (c) χ_{bs}^d , and (d) the correlation between $Re(\epsilon'_K/\epsilon_K)_{H^\pm}$ and $\epsilon_K^{S+H^\pm}$ (in units of 10^{-3}).

E. Charged-Higgs contributions to $K \rightarrow \pi\nu\bar{\nu}$

In this subsection, we discuss the charged-Higgs contributions to the $K^+ \rightarrow \pi^+\nu\bar{\nu}$ and $K_L \rightarrow \pi^0\nu\bar{\nu}$ processes. As mentioned before, the $W^\pm H^\pm$ and $G^\pm H^\pm$ box diagrams are suppressed by $m_\tau^2/m_W^2\zeta_\tau^\ell t_\beta$, where although there is a t_β enhancement factor, their contributions are still small and negligible. The Wilson coefficient from the $H^\pm H^\pm$ box diagram can be enhanced through the $(\zeta_\tau^\ell t_\beta)^2$ factor; however, its sign is opposite to that of the SM, so that it has a destructive effect on the SM results. Thus, we cannot rely on $H^\pm H^\pm$ to enhance $BR(K^+ \rightarrow \pi^+\nu\bar{\nu})$ and $BR(K_L \rightarrow \pi^0\nu\bar{\nu})$. Hence, the main charged-Higgs effect on

the $d \rightarrow s\nu\bar{\nu}$ process is derived from the Z -penguin diagram.

With the input parameter values, the BRs for the $K^+ \rightarrow \pi^+\nu\bar{\nu}$ and $K_L \rightarrow \pi^0\nu\bar{\nu}$ processes in the SM can be estimated to be $BR(K^+ \rightarrow \pi^+\nu\bar{\nu}) \approx 8.8 \times 10^{-11}$ and $BR(K_L \rightarrow \pi^0\nu\bar{\nu}) \approx 2.9 \times 10^{-11}$. Using the parameter values, which are constrained by the B -meson and K -meson data, we calculate the charged-Higgs contributions to $K^+ \rightarrow \pi^+\nu\bar{\nu}$ and $K_L \rightarrow \pi^0\nu\bar{\nu}$, where the BRs (in units of 10^{-11}) as a function of χ_{ct}^u are shown in Fig. 9(a) and (b). In order to suppress the contribution from the $H^\pm H^\pm$ diagram, we take $\chi_\tau^\ell = 1$. From the plots, we clearly see that $BR(K^+ \rightarrow \pi^+\nu\bar{\nu})$ can be enhanced to $\sim 13 \times 10^{-11}$ while $BR(K_L \rightarrow \pi^0\nu\bar{\nu})$ is enhanced to $\sim 3.6 \times 10^{-11}$. Since the CP violating source in the charged-Higgs loop is the same as that of the SM, the $K_L \rightarrow \pi^0\nu\bar{\nu}$ enhancement is limited. Although the charged-Higgs cannot enhance $K^+ \rightarrow \pi^+\nu\bar{\nu}$ by a factor of 2, it can increase the SM result by 60%. For clarity, we show the correlation between $BR(K^+ \rightarrow \pi^+\nu\bar{\nu})$ and $BR(K_L \rightarrow \pi^0\nu\bar{\nu})$ in Fig. (10). In addition, the correlations between the rare K decays and $(\epsilon'_K/\epsilon_K)_{H^\pm}$ are also given in Fig. 11(a) and (b).

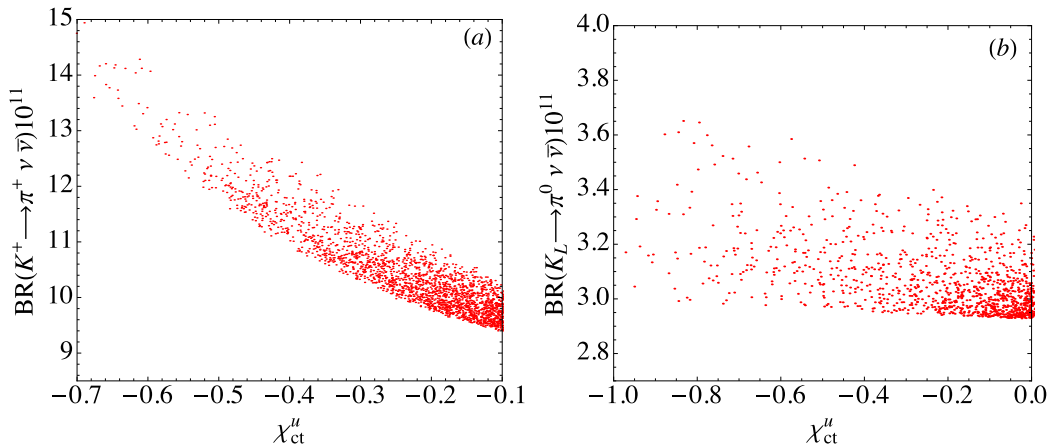


FIG. 9: (a) $BR(K^+ \rightarrow \pi^+\nu\bar{\nu})$ and (b) $BR(K_L \rightarrow \pi^0\nu\bar{\nu})$ as a function of χ_{ct}^u .

VI. CONCLUSION

We comprehensively studied the $Re(\epsilon'_K/\epsilon_K)$ and the rare $K^+(K_L) \rightarrow \pi^+(\pi^0)\nu\bar{\nu}$ decays in the type-III 2HDM, where the Cheng-Sher ansatz was applied, and the main CP-violation phase was still from the CKM matrix element V_{td} when the Wolfenstein parametrization was taken. We used $|\Delta M_K^{\text{NP}}| < 0.2\Delta M_K^{\text{exp}}$ and $|\epsilon_K^{\text{NP}}| < 0.4 \times 10^{-3}$ to bound the free parameters.

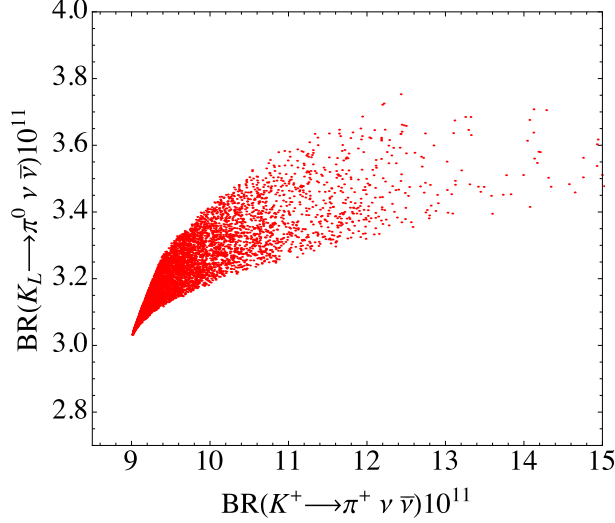


FIG. 10: Correlation between $BR(K^+ \rightarrow \pi^+ \nu \bar{\nu})$ and $BR(K_L \rightarrow \pi^0 \nu \bar{\nu})$.

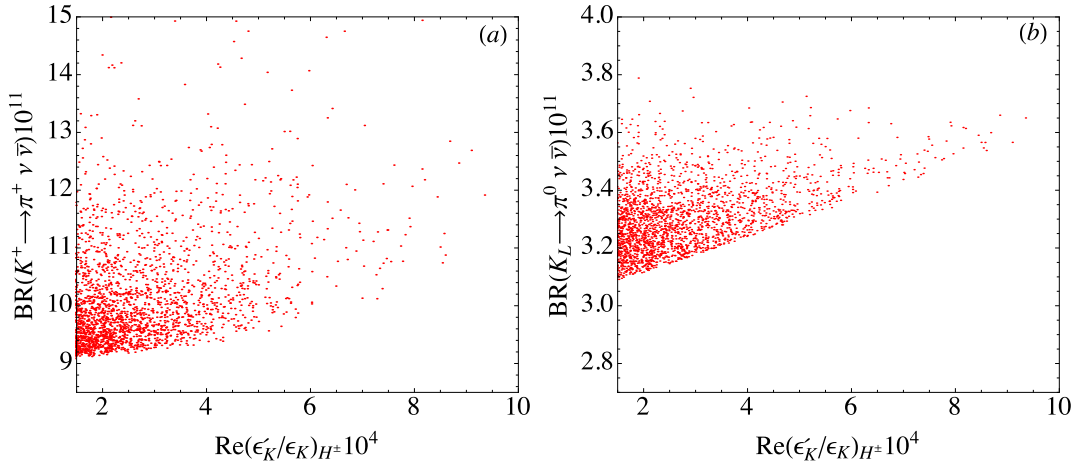


FIG. 11: Correlation between $(\epsilon'_K/\epsilon_K)_{H^\pm}$ and (a) $BR(K^+ \rightarrow \pi^+ \nu \bar{\nu})$ and (b) $BR(K_L \rightarrow \pi^0 \nu \bar{\nu})$.

The charged-Higgs related parameters, which contribute to ΔM_K and ϵ_K , also contribute to $\Delta M_{B_d, B_s}$ and $B \rightarrow X_s \gamma$ processes. When the constraints from the K and B systems are satisfied, we found that it is possible to obtain $(\epsilon'_K/\epsilon_K)_{H^\pm} \sim 8 \times 10^{-4}$ in the generic 2HDM, where the dominant effective operator is from the electroweak penguin Q_8 .

The dominant contribution to the rare $K \rightarrow \pi \nu \bar{\nu}$ decays in the type-III 2HDM is the H^\pm -loop Z -penguin diagram. With the same set of constrained parameters, we found that $K_L \rightarrow \pi^0 \nu \bar{\nu}$ can be slightly enhanced to $BR(K_L \rightarrow \pi^0 \nu \bar{\nu}) \sim 3.6 \times 10^{-11}$, whereas $K^+ \rightarrow \pi^+ \nu \bar{\nu}$ can be enhanced to $BR(K^+ \rightarrow \pi^+ \nu \bar{\nu}) \sim 13 \times 10^{-11}$. Although the BRs of the rare $K \rightarrow \pi \nu \bar{\nu}$ decays cannot be enhanced by one order of magnitude in the type-III 2HDM, the

results are still located within the detection level in the KOTO experiment at J-PARC and the NA62 experiment at CERN.

Acknowledgments

This work was partially supported by the Ministry of Science and Technology of Taiwan, under grants MOST-106-2112-M-006-010-MY2 (CHC).

-
- [1] B. Aubert *et al.* [BaBar Collaboration], Phys. Rev. Lett. **86**, 2515 (2001) [hep-ex/0102030].
 - [2] A. Abashian *et al.* [Belle Collaboration], Phys. Rev. Lett. **86**, 2509 (2001) [hep-ex/0102018].
 - [3] N. Cabibbo, Phys. Rev. Lett. **10**, 531 (1963).
 - [4] M. Kobayashi and T. Maskawa, Prog. Theor. Phys. **49**, 652 (1973).
 - [5] P. A. Boyle *et al.* [RBC and UKQCD Collaborations], Phys. Rev. Lett. **110**, no. 15, 152001 (2013) [arXiv:1212.1474 [hep-lat]].
 - [6] T. Blum *et al.*, Phys. Rev. Lett. **108**, 141601 (2012) [arXiv:1111.1699 [hep-lat]].
 - [7] T. Blum *et al.*, Phys. Rev. D **86**, 074513 (2012) [arXiv:1206.5142 [hep-lat]].
 - [8] T. Blum *et al.*, Phys. Rev. D **91**, no. 7, 074502 (2015) [arXiv:1502.00263 [hep-lat]].
 - [9] Z. Bai *et al.* [RBC and UKQCD Collaborations], Phys. Rev. Lett. **115**, no. 21, 212001 (2015) [arXiv:1505.07863 [hep-lat]].
 - [10] J. R. Batley *et al.* [NA48 Collaboration], Phys. Lett. B **544**, 97 (2002) [hep-ex/0208009].
 - [11] A. Alavi-Harati *et al.* [KTeV Collaboration], Phys. Rev. D **67**, 012005 (2003) Erratum: [Phys. Rev. D **70**, 079904 (2004)] [hep-ex/0208007].
 - [12] E. Abouzaid *et al.* [KTeV Collaboration], Phys. Rev. D **83**, 092001 (2011) [arXiv:1011.0127 [hep-ex]].
 - [13] A. J. Buras and J. M. Gerard, JHEP **1512**, 008 (2015) [arXiv:1507.06326 [hep-ph]].
 - [14] A. J. Buras, M. Gorbahn, S. Jager and M. Jamin, JHEP **1511**, 202 (2015) [arXiv:1507.06345 [hep-ph]].
 - [15] A. J. Buras and J. M. Gerard, Nucl. Phys. B **264**, 371 (1986).
 - [16] W. A. Bardeen, A. J. Buras and J. M. Gerard, Phys. Lett. B **180**, 133 (1986).
 - [17] W. A. Bardeen, A. J. Buras and J. M. Gerard, Nucl. Phys. B **293**, 787 (1987).

- [18] W. A. Bardeen, A. J. Buras and J. M. Gerard, Phys. Lett. B **192**, 138 (1987).
- [19] W. A. Bardeen, A. J. Buras and J. M. Gerard, Phys. Lett. B **211**, 343 (1988).
- [20] A. J. Buras and J. M. Gerard, Eur. Phys. J. C **77**, no. 1, 10 (2017) [arXiv:1603.05686 [hep-ph]].
- [21] A. J. Buras and J. M. Gerard, arXiv:1803.08052 [hep-ph].
- [22] H. Gisbert and A. Pich, arXiv:1712.06147 [hep-ph].
- [23] A. J. Buras, D. Buttazzo, J. Girrbach-Noe and R. Knegjens, JHEP **1511**, 033 (2015) [arXiv:1503.02693 [hep-ph]].
- [24] A. J. Buras, D. Buttazzo and R. Knegjens, JHEP **1511**, 166 (2015) [arXiv:1507.08672 [hep-ph]].
- [25] A. J. Buras and F. De Fazio, JHEP **1603**, 010 (2016) [arXiv:1512.02869 [hep-ph]].
- [26] A. J. Buras, JHEP **1604**, 071 (2016) [arXiv:1601.00005 [hep-ph]].
- [27] M. Tanimoto and K. Yamamoto, PTEP **2016**, no. 12, 123B02 (2016) [arXiv:1603.07960 [hep-ph]].
- [28] A. J. Buras and F. De Fazio, JHEP **1608**, 115 (2016) [arXiv:1604.02344 [hep-ph]].
- [29] T. Kitahara, U. Nierste and P. Tremper, Phys. Rev. Lett. **117**, no. 9, 091802 (2016) [arXiv:1604.07400 [hep-ph]].
- [30] M. Endo, S. Mishima, D. Ueda and K. Yamamoto, Phys. Lett. B **762**, 493 (2016) [arXiv:1608.01444 [hep-ph]].
- [31] C. Bobeth, A. J. Buras, A. Celis and M. Jung, JHEP **1704** (2017) 079 doi:10.1007/JHEP04(2017)079 [arXiv:1609.04783 [hep-ph]].
- [32] V. Cirigliano, W. Dekens, J. de Vries and E. Mereghetti, Phys. Lett. B **767**, 1 (2017) [arXiv:1612.03914 [hep-ph]].
- [33] M. Endo, T. Kitahara, S. Mishima and K. Yamamoto, Phys. Lett. B **771**, 37 (2017) [arXiv:1612.08839 [hep-ph]].
- [34] C. Bobeth, A. J. Buras, A. Celis and M. Jung, JHEP **1707**, 124 (2017) [arXiv:1703.04753 [hep-ph]].
- [35] A. Crivellin, G. D'Ambrosio, T. Kitahara and U. Nierste, Phys. Rev. D **96**, no. 1, 015023 (2017) [arXiv:1703.05786 [hep-ph]].
- [36] C. Bobeth and A. J. Buras, JHEP **1802**, 101 (2018) [arXiv:1712.01295 [hep-ph]].
- [37] N. Haba, H. Umeeda and T. Yamada, arXiv:1802.09903 [hep-ph].

- [38] G. Buchalla and A. J. Buras, Nucl. Phys. B **400**, 225 (1993).
- [39] M. Misiak and J. Urban, Phys. Lett. B **451**, 161 (1999) [hep-ph/9901278].
- [40] G. Buchalla and A. J. Buras, Nucl. Phys. B **548**, 309 (1999) [hep-ph/9901288].
- [41] M. Gorbahn and U. Haisch, Nucl. Phys. B **713**, 291 (2005) [hep-ph/0411071].
- [42] A. J. Buras, M. Gorbahn, U. Haisch and U. Nierste, Phys. Rev. Lett. **95**, 261805 (2005) [hep-ph/0508165].
- [43] A. J. Buras, M. Gorbahn, U. Haisch and U. Nierste, JHEP **0611**, 002 (2006) Erratum: [JHEP **1211**, 167 (2012)] [hep-ph/0603079].
- [44] G. Buchalla and A. J. Buras, Phys. Rev. D **57**, 216 (1998) [hep-ph/9707243].
- [45] J. Brod and M. Gorbahn, Phys. Rev. D **78**, 034006 (2008) [arXiv:0805.4119 [hep-ph]].
- [46] J. Brod, M. Gorbahn and E. Stamou, Phys. Rev. D **83**, 034030 (2011) [arXiv:1009.0947 [hep-ph]].
- [47] F. Newson *et al.*, arXiv:1411.0109 [hep-ex].
- [48] M. Moulson [NA62 Collaboration], PoS ICHEP **2016**, 581 (2016) [arXiv:1611.04979 [hep-ex]].
- [49] T. K. Komatsubara, Prog. Part. Nucl. Phys. **67**, 995 (2012) [arXiv:1203.6437 [hep-ex]].
- [50] B. Beckford [KOTO Collaboration], arXiv:1710.01412 [hep-ex].
- [51] A. V. Artamonov *et al.* [E949 Collaboration], Phys. Rev. Lett. **101**, 191802 (2008) [arXiv:0808.2459 [hep-ex]].
- [52] J. K. Ahn *et al.* [E391a Collaboration], Phys. Rev. D **81**, 072004 (2010) [arXiv:0911.4789 [hep-ex]].
- [53] J. Pinzino *et al.* [NA62 Collaboration], arXiv:1807.09101 [hep-ex].
- [54] T. P. Cheng and M. Sher, Phys. Rev. D **35**, 3484 (1987).
- [55] G. 't Hooft, Naturalness, chiral symmetry, and spontaneous chiral symmetry breaking, NATO Sci. Ser. B **59**, 135 (1980).
- [56] A. Crivellin, A. Kokulu and C. Greub, Phys. Rev. D **87**, no. 9, 094031 (2013) [arXiv:1303.5877 [hep-ph]].
- [57] M. Misiak and M. Steinhauser, Eur. Phys. J. C **77**, no. 3, 201 (2017) [arXiv:1702.04571 [hep-ph]].
- [58] C. H. Chen and T. Nomura, arXiv:1803.00171 [hep-ph].
- [59] C. H. Chen and T. Nomura, Eur. Phys. J. C **77**, no. 9, 631 (2017) [arXiv:1703.03646 [hep-ph]].
- [60] R. Dutta, A. Bhol and A. K. Giri, Phys. Rev. D **88**, no. 11, 114023 (2013) [arXiv:1307.6653

- [hep-ph]].
- [61] B. Bhattacharya, A. Datta, D. London and S. Shivashankara, Phys. Lett. B **742**, 370 (2015) [arXiv:1412.7164 [hep-ph]].
- [62] B. Bhattacharya, A. Datta, J. P. Guevin, D. London and R. Watanabe, JHEP **1701**, 015 (2017) [arXiv:1609.09078 [hep-ph]].
- [63] R. Dutta and A. Bhol, Phys. Rev. D **96**, no. 3, 036012 (2017) [arXiv:1611.00231 [hep-ph]].
- [64] S. Bhattacharya, S. Nandi and S. K. Patra, Phys. Rev. D **95**, no. 7, 075012 (2017) [arXiv:1611.04605 [hep-ph]].
- [65] R. Dutta and A. Bhol, Phys. Rev. D **96**, no. 7, 076001 (2017) [arXiv:1701.08598 [hep-ph]].
- [66] A. G. Akeroyd and C. H. Chen, Phys. Rev. D **96**, no. 7, 075011 (2017) [arXiv:1708.04072 [hep-ph]].
- [67] A. Arhrib, R. Benbrik, C. H. Chen, J. K. Parry, L. Rahili, S. Semlali and Q. S. Yan, arXiv:1710.05898 [hep-ph].
- [68] C. Patrignani *et al.* (Particle Data Group), Chin. Phys. C **40**, 100001 (2016).
- [69] A. J. Buras, S. Jager and J. Urban, Nucl. Phys. B **605**, 600 (2001) [hep-ph/0102316].
- [70] V. Cirigliano, G. Ecker, H. Neufeld, A. Pich and J. Portoles, Rev. Mod. Phys. **84**, 399 (2012) [arXiv:1107.6001 [hep-ph]].
- [71] V. Cirigliano, G. Ecker, H. Neufeld and A. Pich, Eur. Phys. J. C **33**, 369 (2004) [hep-ph/0310351].
- [72] A. J. Buras, M. Jamin and M. E. Lautenbacher, Nucl. Phys. B **408**, 209 (1993) [hep-ph/9303284].
- [73] A. J. Buras, J. M. Gerard and W. A. Bardeen, Eur. Phys. J. C **74**, 2871 (2014) [arXiv:1401.1385 [hep-ph]].
- [74] A. J. Davies, G. C. Joshi and M. Matsuda, Phys. Rev. D **44**, 2114 (1991).
- [75] A. J. Buras, P. Gambino, M. Gorbahn, S. Jager and L. Silvestrini, Nucl. Phys. B **592**, 55 (2001) [hep-ph/0007313].
- [76] G. Isidori, F. Mescia and C. Smith, Nucl. Phys. B **718**, 319 (2005) [hep-ph/0503107].
- [77] F. Mescia and C. Smith, Phys. Rev. D **76**, 034017 (2007) [arXiv:0705.2025 [hep-ph]].
- [78] J. Brod and M. Gorbahn, Phys. Rev. D **82**, 094026 (2010) [arXiv:1007.0684 [hep-ph]].
- [79] G. Buchalla, A. J. Buras and M. E. Lautenbacher, Rev. Mod. Phys. **68**, 1125 (1996) [hep-ph/9512380].

- [80] T. Bae *et al.*, PoS LATTICE **2013**, 476 (2014) [arXiv:1310.7319 [hep-lat]].
- [81] J. Frison *et al.* [RBC-UKQCD Collaboration], PoS LATTICE **2013**, 460 (2014) [arXiv:1312.2374 [hep-lat]].
- [82] S. Herrlich and U. Nierste, Nucl. Phys. B **419**, 292 (1994) [hep-ph/9310311].
- [83] J. Brod and M. Gorbahn, Phys. Rev. Lett. **108**, 121801 (2012) [arXiv:1108.2036 [hep-ph]].
- [84] L. Wolfenstein, Phys. Rev. Lett. **51**, 1945 (1983).
- [85] Y. Amhis *et al.* [HFLAV Collaboration], Eur. Phys. J. C **77**, no. 12, 895 (2017) [arXiv:1612.07233 [hep-ex]].
- [86] M. E. Peskin and T. Takeuchi, Phys. Rev. D **46**, 381 (1992).
- [87] R. Benbrik, C. H. Chen and T. Nomura, Phys. Rev. D **93**, no. 9, 095004 (2016) [arXiv:1511.08544 [hep-ph]].
- [88] V. Khachatryan *et al.* [CMS Collaboration], JHEP **1511**, 018 (2015) [arXiv:1508.07774 [hep-ex]].
- [89] M. Krawczyk, S. Moretti, P. Osland, G. Pruna and R. Santos, J. Phys. Conf. Ser. **873**, no. 1, 012048 (2017) [arXiv:1703.05925 [hep-ph]].
- [90] J. L. Diaz-Cruz and O. A. Sampayo, Phys. Rev. D **50**, 6820 (1994).
- [91] F. Borzumati, J. L. Kneur and N. Polonsky, Phys. Rev. D **60**, 115011 (1999) [hep-ph/9905443].
- [92] A. G. Akeroyd *et al.*, Eur. Phys. J. C **77**, no. 5, 276 (2017) [arXiv:1607.01320 [hep-ph]].
- [93] A. Belyaev, N. D. Christensen and A. Pukhov, Comput. Phys. Commun. **184**, 1729 (2013) [arXiv:1207.6082 [hep-ph]].
- [94] P. M. Nadolsky, H. L. Lai, Q. H. Cao, J. Huston, J. Pumplin, D. Stump, W. K. Tung and C.-P. Yuan, Phys. Rev. D **78**, 013004 (2008) [arXiv:0802.0007 [hep-ph]].
- [95] T. Plehn, Phys. Rev. D **67**, 014018 (2003) [hep-ph/0206121].
- [96] H. E. Logan and U. Nierste, Nucl. Phys. B **586**, 39 (2000) [hep-ph/0004139].
- [97] C. S. Huang, W. Liao, Q. S. Yan and S. H. Zhu, Phys. Rev. D **63**, 114021 (2001) Erratum: [Phys. Rev. D **64**, 059902 (2001)] [hep-ph/0006250].
- [98] P. H. Chankowski and L. Slawianowska, Phys. Rev. D **63**, 054012 (2001) [hep-ph/0008046].
- [99] C. Bobeth, T. Ewerth, F. Kruger and J. Urban, Phys. Rev. D **64**, 074014 (2001) [hep-ph/0104284].
- [100] R. Aaij *et al.* [LHCb Collaboration], Phys. Rev. Lett. **118**, no. 19, 191801 (2017)

[arXiv:1703.05747 [hep-ex]].

- [101] C. Bobeth, M. Gorbahn, T. Hermann, M. Misiak, E. Stamou and M. Steinhauser, Phys. Rev. Lett. **112**, 101801 (2014) [arXiv:1311.0903 [hep-ph]].